Stability and Synchronization of a Ring of Identical Cells with Delayed Coupling

Yuan Yuan
Department of Mathematics and Statistics
Memorial University of Newfoundland
St. John's NL A1C 5S7
Canada
and
Sue Ann Campbell
Department of Applied Mathematics
University of Waterloo
Waterloo, Ontario, N2L 3G1
Canada

June 22, 2004

Abstract

We consider a ring of identical elements with time delayed, nearest neighbour coupling. The individual elements are modelled by a scalar delay differential equation which includes linear decay and nonlinear delayed feedback. The linear stability of the trivial solution is completely analyzed and illustrated in the parameter space of the coupling strength and the coupling delay. Conditions for global stability of the trivial solution are also given. The bifurcation and stability of nontrivial synchronous solutions from the trivial solution is analyzed using a centre manifold construction.

Keywords: **delay differential equations, neural networks, stability, D^n symmetry, synchronization**

1 Introduction

The work of Golubitsky, Stewart and Schaeffer [9, Chapter XVIII], shows that rings of identical cells can lead to many interesting patterns of oscillation, which are predictable

based on the theory of equivariant bifurcations. In a series of papers [18, 19, 26] Wu et al. extended the theory of equivariant Hopf bifurcation to delay differential equations. Recently, there has been interest in applying these results to neural networks, primarily to models related to the Hopfield-Cohen-Grossberg neural networks [6, 10, 11, 15, 16] with time delays [20, 21]. Most of these studies have concerned lower dimensional systems (e.g [2, 22, 27]) and/or systems with a single time delay [26, 27].

In this paper, we consider the generalization to arbitrary n of the model studied by [4, 22]. That is, we consider system of n identical elements with time delayed nearest-neighbour coupling. The individual elements are represented by a scalar equation, consisting of a linear decay term and a nonlinear, time delayed self connection (feedback). The architecture of the model is given in Figure 1.

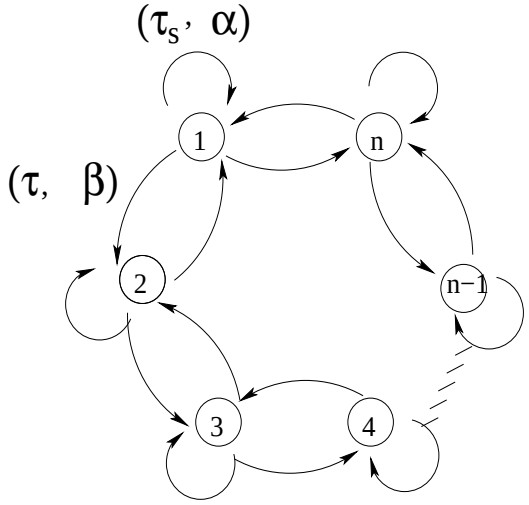

Figure 1: Architecture of a network of n neurons with two different time delays

This model can be described by the following delay differential equations:

$$\dot{x_i}(t) = -x_i(t) + \alpha\, f(x_i(t-\tau_s)) + \beta\left[g(x_{i-1}(t-\tau)) + g(x_{i+1}(t-\tau))\right], \qquad (i \bmod n) \tag{1}$$

where $f\,, g$ are adequately smooth, e.g. $f,\, g \in C^3$, and satisfy the following normalization, monotonicity, concavity and boundedness conditions:

(C1) $f(0) = g(0) = 0, f'(0) = g'(0) = 1,$ and $f'(x) > 0,\ g'(x) > 0$ for all $x \in \mathbb{R}$;

(C2) $x\, f''(x) < 0$ and $x\, g''(x) < 0$ for all $x \neq 0$;

(C3) $-\infty < \lim_{x\to\pm\infty} f(x),\ g(x) < \infty$;

(C4) $f'''(0) < 0\,, g'''(0) < 0$.

Remark 1.1 *i) For example, we can choose $f(x) = g(x) = \tanh(x)$, which we will do for the numerical simulations and the center manifold construction.*
ii) The model clearly possesses D^n symmetry.
iii) Note that when $n = 2$, the model is not in the "natural" setup, however, it can be transformed to this by scaling 2β to β.

We note that, when isolated, the individual elements satisfy the scalar delay differential equation

$$\dot{x_i}(t) = -x_i(t) + \alpha\, f(x_i(t - \tau_s)). \tag{2}$$

It is well known (see e.g. [2]) that for f satisfying conditions such as those above, the trivial solution always exists and is locally stable if

$$\begin{aligned} -1 < \alpha < 1 \quad &\text{and} \quad \tau_s > 0 \\ \alpha < -1 \quad &\text{and} \quad \tau_s < \tfrac{1}{\sqrt{\alpha^2-1}} \operatorname{Arccos}(\tfrac{1}{\alpha}) \stackrel{def}{=} \tau_s^H \end{aligned} \tag{3}$$

Further, there is a steady state bifurcation at $\alpha = 1$ and a Hopf bifurcation at $\tau = \tau_s^H$ when $\alpha < -1$. We can thus consider our model as a system of n coupled oscillators with time delayed, nearest neighbour coupling.

Let $h = \max\{\tau, \tau_s\}$ and denote by $\mathcal{C}$ the Banach space of continuous mappings from $[-h, 0]$ to $\mathbb{R}^n$ equipped with the usual super-norm. Let $x(t)$ be a solution of (1) and define $x_t(\theta) = x(t + \theta),\ -h \leq \theta \leq 0$. If $x(t)$ is continuous, then $x_t(\theta) \in \mathcal{C}$. $\mathcal{C}$ is the standard phase space of the semiflow defined by equation (1).

There are two main goals of this paper: (i) to study the local stability of the trivial solution of (1); (ii) to study the existence and stability of synchronized solutions of (1).

The former is the content of Sections 2-5, the latter of sections 6 and 7. Section 2 derives the characteristic equation of the linearization of (1) about the trivial solution. Section 3 uses this to derive some local stability results which are independent of one or both of the delays. Section 4 determines curves, in the β, τ plane, along which the characteristic equation has a zero root or pair of pure imaginary roots, and describes how the geometry of these curves changes as the parameters α and τ_s are varied. Section 5 uses these results to give a complete description of the region of linear stability of the trivial solution of (1). Section 6 uses Lyapunov functionals to establish global stability and synchronization conditions for (1). Section 7 studies the bifurcation of nontrivial synchronous solutions from the trivial solution. Finally, Section 8 presents a summary of our current work and a discussion of future work.

2 Characteristic Equation

The linearization of (1) at the equilibrium point $(x^*, x^*, \ldots, x^*)$ is

$$\dot{u}_i(t) = -\,u_i(t) + \alpha\, f'(x^*)\, u_i(t-\tau_s) + \beta\, g'(x^*)[u_{i-1}(t-\tau) + u_{i+1}(t-\tau)\,] \qquad (i \bmod n)\,. \tag{4}$$

In vector form, this can be written as

$$\dot{u}(t) = -\,I\,u(t) \,+\, \alpha\, f'(x^*)\, I\, u(t-\tau_s) \,+\, \beta\, g'(x^*)\, M\, u(t-\tau)\,, \tag{5}$$

where I is $n \times n$ identity matrix and

$$M = \begin{pmatrix} 0 & 1 & 0 & \cdots & 1 \\ 1 & 0 & 1 & \cdots & 0 \\ 0 & 1 & 0 & \cdots & 0 \\ \vdots & \vdots & \vdots & \cdots & \vdots \\ 1 & 0 & 0 & \cdots & 0 \end{pmatrix}_{n\times n} . \tag{6}$$

From condition (C1) it is clear that (1) admits the trivial solution, $x^* = 0$. The characteristic matrix of the linearization of (1) at this equilibrium is

$$\mathcal{M}_n(0,\, \lambda) = (\lambda \,+\, 1 \,-\, \alpha\, e^{-\lambda\,\tau_s})\, I \,-\, \beta\, e^{-\lambda\,\tau}\, M\,. \tag{7}$$

Let

$$\chi = e^{\frac{2\pi}{n}\,i}, \qquad v_j = (1,\, \chi^j,\, \chi^{2j},\, \ldots,\, \chi^{(n-1)j}) \quad (j = 0, 1, \ldots, n-1)\,. \tag{8}$$

Since

$$\begin{aligned}
\chi^{nj} &= e^{2\pi\, j\, i} = 1\,, \\
\chi^{(n-1)j} &= e^{\frac{2\pi(n-1)}{n}\, j\, i} = e^{(2\pi - \frac{2\pi}{n}) j\, i} = e^{-\frac{2\pi\, j}{n} i} = \chi^{-j}\,, \\
\chi^{(n-2)j} &= e^{\frac{2\pi(n-2)}{n}\, j\, i} = e^{(2\pi - \frac{4\pi}{n}) j\, i} = e^{-\frac{4\pi\, j}{n} i} = \chi^{-2j}\,, \\
&\vdots
\end{aligned}$$

It follows that

$$M\, v_j = \begin{pmatrix} \chi^j + \chi^{(n-1)j} \\ 1 + \chi^{2j} \\ \chi^j + \chi^{3j} \\ \vdots \\ 1 + \chi^{(n-2)j} \end{pmatrix} = (\chi^j + \chi^{-j})\, v_j\,. \tag{9}$$

Hence,

$$\begin{aligned}
\mathcal{M}_n(0,\, \lambda)\, v_j &= (\lambda + 1 - \alpha\, e^{-\lambda\, \tau_s} - \beta\, e^{-\lambda\, \tau}\, (\chi^j + \chi^{-j}))\, v_j \\
&= (\lambda + 1 - \alpha\, e^{-\lambda\, \tau_s} - 2\, \beta\, e^{-\lambda\, \tau}\, \cos\frac{2\pi\, j}{n})\, v_j\,,
\end{aligned} \tag{10}$$

and the characteristic equation is

$$\begin{aligned}
\det \mathcal{M}_n(0,\, \lambda) &= \prod_{j=0}^{n-1} (\lambda + 1 - \alpha\, e^{-\lambda\, \tau_s} - 2\, \beta\, e^{-\lambda\, \tau}\, \cos\frac{2\pi\, j}{n}) \\
&= (a - 2b) \prod_{j=1}^{n-1} (a - 2\, b\, \cos\frac{2\pi\, j}{n}) = 0\,,
\end{aligned} \tag{11}$$

where

$$a = \lambda + 1 - \alpha\, e^{-\lambda\, \tau_s}, \qquad b = \beta\, e^{-\lambda\, \tau}\,. \tag{12}$$

We observe that eq. (12) can be simplified, further elucidating the structure of the characteristic equation. When n is an odd number, we obtain

$$\begin{aligned}
\det \mathcal{M}_n(0,\,\lambda) &= (a-2b)\,[\,(a-2\,b\,\cos\frac{2\pi}{n})\,(a-2\,b\,\cos\frac{4\pi}{n})\,\cdots\,(a-2\,b\,\cos\frac{(n-1)\pi}{n})\,]^2 \\
&= \Delta_0(\lambda)\prod_{j=1}^{\frac{n-1}{2}}\Delta_j^2(\lambda) \\
&= (\lambda+1-\alpha e^{-\lambda\tau_s}-2\beta e^{-\lambda\tau})\prod_{j=1}^{\frac{n-1}{2}}(\lambda+1-\alpha e^{-\lambda\tau_s}-2\beta e^{-\lambda\tau}\cos\frac{2\pi j}{n})^2\,, \quad (13)
\end{aligned}$$

whereas when n is an even number, we obtain

$$\begin{aligned}
\det \mathcal{M}_n(0,\,\lambda) &= (a-2b)\,(a+2b)[\,(a-2\,b\,\cos\frac{2\pi}{n})\,(a-2\,b\,\cos\frac{4\pi}{n})\,\cdots\,(a-2\,b\,\cos\frac{(n-2)\pi}{n})\,]^2 \\
&= \Delta_0(\lambda)\Delta_{\frac{n}{2}}(\lambda)\prod_{j=1}^{\frac{n}{2}-1}\Delta_j^2(\lambda) \\
&= (\lambda+1-\alpha e^{-\lambda\tau_s}-2\beta e^{-\lambda\tau})(\lambda+1-\alpha e^{-\lambda\tau_s}+2\beta e^{-\lambda\tau}) \\
&\quad \prod_{j=1}^{\frac{n}{2}-1}(\lambda+1-\alpha e^{-\lambda\tau_s}-2\beta e^{-\lambda\tau}\cos\frac{2\pi j}{n})^2\,. \quad (14)
\end{aligned}$$

The case when n is even, i.e. $n=2m$, may be further simplified into two subcases. When m is an odd number we have

$$\begin{aligned}
\det \mathcal{M}_n(0,\,\lambda) &= \Delta_0(\lambda)\Delta_{\frac{n}{2}}(\lambda)\prod_{j=1}^{\frac{m-1}{2}}\Delta_j^2(\lambda)\Delta_{m-j}^2(\lambda) \quad (15) \\
&= (\lambda+1-\alpha e^{-\lambda\tau_s}-2\beta e^{-\lambda\tau})(\lambda+1-\alpha e^{-\lambda\tau_s}+2\beta e^{-\lambda\tau}) \\
&\quad \prod_{j=1}^{\frac{m-1}{2}}(\lambda+1-\alpha e^{-\lambda\tau_s}-2\beta e^{-\lambda\tau}\cos\frac{\pi j}{m})^2(\lambda+1-\alpha e^{-\lambda\tau_s}+2\beta e^{-\lambda\tau}\cos\frac{\pi j}{m})^2\,.
\end{aligned}$$

whereas when m is an even number we have

$$\begin{aligned}
\det \mathcal{M}_n(0,\,\lambda) &= \Delta_0(\lambda)\Delta_{\frac{n}{2}}(\lambda)\Delta_{\frac{n}{4}}^2(\lambda)\prod_{j=1}^{\frac{m}{2}-1}\Delta_j^2(\lambda)\Delta_{m-j}^2(\lambda) \quad (16) \\
&= (\lambda+1-\alpha e^{-\lambda\tau_s}-2\beta e^{-\lambda\tau})(\lambda+1-\alpha e^{-\lambda\tau_s}+2\beta e^{-\lambda\tau})(\lambda+1-\alpha e^{-\lambda\tau_s})^2 \\
&\quad \prod_{j=1}^{\frac{m}{2}-1}(\lambda+1-\alpha e^{-\lambda\tau_s}-2\beta e^{-\lambda\tau}\cos\frac{\pi j}{m})^2(\lambda+1-\alpha e^{-\lambda\tau_s}+2\beta e^{-\lambda\tau}\cos\frac{\pi j}{m})^2\,.
\end{aligned}$$

3 Delay Independent Linear Stability Results

Recall that an equilibrium solution of a delay differential equation is locally asymptotically stable if all the roots of the corresponding characteristic equation have negative real parts and unstable if at least one root has positive real part [14, 17]. Based on this result and the expression for characteristic equation of the trivial solution of (1) obtained in the last section, we will develop three results which are independent of one or both of the delays τ, τ_s. These describe subsets of the full region of linear stability. The proofs of the theorems are extensions of those found in [4] for the case $n = 3$, [23] for the case $n = 2$ with no symmetry and [1] for the case $n = 1$.

Theorem 3.1 *If the parameters satisfy* $|\beta| < \frac{1}{2}(1 - |\alpha|)$*, the trivial solution of (1) is locally asymptotically stable for all* $\tau_s \geq 0$ *and* $\tau \geq 0$*.*

Proof. From (13) and (14) for each $\Delta_j(\lambda)\,,\ (j = 0,\, 1,\, \cdots,\, [\frac{n}{2}])^{\dagger}$ we have

$$\Delta_j(\lambda) = a - 2\,b\,\cos\frac{2\pi\,j}{n} = \lambda + 1 - \alpha\,e^{-\lambda\,\tau_s} - 2\,\beta\,e^{-\lambda\,\tau}\,\cos\frac{2\pi\,j}{n}\,. \tag{17}$$

Let $\lambda = v + i\,w,\ \ v, w \in \mathbb{R}$, and $\Delta_j(\lambda) = R_j(v,\, w) + i\,I_j(v,\, w)$, then

$$\begin{aligned} R_j(v,\, w) &= v + 1 - \alpha\,e^{-v\tau_s}\cos(w\tau_s) - 2\beta\,e^{-v\tau}\,\cos\frac{2\pi\,j}{n}\,\cos(w\tau)\,, \\ I_j(v,\, w) &= w + \alpha\,e^{-v\tau_s}\sin(w\tau_s) + 2\beta\,e^{-v\tau}\,\cos\frac{2\pi\,j}{n}\,\sin(w\tau)\,. \end{aligned} \tag{18}$$

Therefore, one can obtain

$$R_j(v,\, w) \geq v + 1 - |\alpha|\,e^{-v\tau_s} - 2\,|\beta|\,e^{-v\tau}\,. \tag{19}$$

Denoting the right-hand side of (19) by $R(v)$, it is easy to see that

$$R(0) = 1 - |\alpha| - 2\,|\beta| > 0 \tag{20}$$

under the assumption of the theorem. In addition,

$$\frac{dR}{dv} = 1 + |\alpha|\,\tau_s\,e^{-v\tau_s} + 2\,|\beta|\,\tau\,e^{-v\tau} > 0\,, \tag{21}$$

$^{\dagger}[m]$ denotes the integer part of m.

so $R(v) > 0$ for all $v \geq 0$, and $R_j(v,\, w) > 0$ for all $v \geq 0$, $w \in \mathbb{R}$.

Now let $\lambda = v + i\, w$ be an arbitrary root of the characteristic equation, then $R_j(v,\, w) = I_j(v,\, w) = 0$. It follows from the discussion above that $v < 0$. Therefore all roots of the characteristic equation have negative real parts, which means that the trivial solution of (1) is locally asymptotically stable for any delay $\tau_s \geq 0$ and $\tau \geq 0$.

Remark 3.1 *Note that this theorem includes the result for the uncoupled oscillators, i.e. the trivial solution is locally asymptotically stable when* $\beta = 0,\ |\alpha| < 1$ *and* $\tau_s \geq 0,\ \tau \geq 0$.

Theorem 3.2 *If the parameters satisfy* $\alpha < -1$, $|\beta| < -\frac{\alpha}{2}$, $0 \leq \tau_s < -\frac{1}{2\alpha}$ *and* $\tau \geq 0$, *then all the roots of the characteristic equation (11) have negative real part.*

Proof: From eq. (17), let $\Delta_j(\lambda) = 0$ and $\lambda = v + iw$, then

$$\begin{aligned} v &= -1 + \alpha\, e^{-v\tau_s} \cos(w\tau_s) + 2\beta\, e^{-v\tau}\, \cos\frac{2\pi\, j}{n}\, \cos(w\tau)\,, \\ w &= -\alpha\, e^{-v\tau_s} \sin(w\tau_s) - 2\beta\, e^{-v\tau}\, \cos\frac{2\pi\, j}{n}\, \sin(w\tau)\,. \end{aligned} \tag{22}$$

Rearranging, squaring and adding these two equations yields a necessary condition for existence of such v and w

$$(v+1)^2 + w^2 - 2\alpha e^{-v\tau_s}[(v+1)\cos(w\tau_s) - w\sin(w\tau_s)] + \alpha^2 e^{-2v\tau_s} - 4\beta^2 e^{-2v\tau}\cos^2\frac{2\pi j}{n} = 0. \tag{23}$$

Denoting the left-hand side of (23) by $M(v)$, we have

$$\begin{aligned} M(0) &= 1 - 2\alpha\cos(w\tau_s) + \alpha^2 + w^2 + 2\alpha w\sin(w\tau_s) - 4\beta^2\cos^2\frac{2\pi j}{n} \\ &\geq 1 - 2\alpha\cos(w\tau_s) + \alpha^2 + w^2 + 2\alpha w\sin(w\tau_s) - 4\beta^2\,, \end{aligned} \tag{24}$$

and

$$\begin{aligned} \frac{dM}{dv} &= 2\{4\tau\beta^2 e^{-2v\tau}\cos^2\frac{2\pi j}{n} - \alpha w\tau_s e^{-v\tau_s}\sin(w\tau_s) + (v+1)[1 + \alpha\tau_s e^{-v\tau_s}\cos(w\tau_s)] \\ &\quad -\alpha e^{-v\tau_s}[\cos(w\tau_s) + \alpha\tau_s e^{-v\tau_s}]\}. \end{aligned} \tag{25}$$

The rest of the proof is essentially the same as that found in the proof of [23, Theorem 2] and hence we omit it.

Theorem 3.3 *If the parameters satisfy $\alpha > 1$ and $\beta \in \mathbb{R}$ or $\alpha = 1$ and $\beta \neq 0$, then the trivial solution of (1) is unstable for all $\tau_s \geq 0$ and $\tau \geq 0$.*

Proof. From (17), we have

$$\Delta_j(0) = 1 - \alpha - 2\,\beta\,\cos\frac{2\pi\,j}{n}\,, \qquad (j = 0,\,1,\,\cdots,\,[\tfrac{n}{2}])\,. \tag{26}$$

Note that $\cos\frac{2\pi\,j}{n} \geq 0\,,\ j = 0,\,1,\,\ldots,\,[\frac{n}{4}]$ and $\cos\frac{2\pi\,j}{n} \leq 0\,,$ for $j = [\frac{n}{4}] + 1,\,\ldots,\,[\frac{n}{2}]$. Thus for any value of β there exists a value $\bar{j} \in \{0,\,1,\,\ldots,\,\frac{n}{2}\}$ such that $\Delta_{\bar{j}}(0) < 0$. Further, for $\lambda \in \mathbb{R}$,

$$\lim_{\lambda\to+\infty}\Delta_{\bar{j}}(\lambda) = \lim_{\lambda\to+\infty}(\lambda + 1 - \alpha\,e^{-\lambda\,\tau_s} - 2\,\beta\,e^{-\lambda\,\tau}\,\cos\frac{2\pi\,\bar{j}}{n}) = +\infty\,. \tag{27}$$

Since $\Delta_{\bar{j}}(\lambda)$ is a continuous function, there exists a $\lambda^* \in (0,\,+\infty)$ such that $\Delta_{\bar{j}}(\lambda^*) = 0$. Thus the characteristic equation has a positive real root for all β under the conditions $\tau_s \geq 0$, $\tau \geq 0$ and $\alpha > 1$. The proof for $\alpha = 1$ and $\beta \neq 0$ is similar.

4 Curves of Characteristic Roots with Zero Real Part

As the parameters are varied, stability may be lost by a real root of the characteristic equation passing through zero or by a pair of complex conjugate roots passing through the imaginary axis. To determine the full region of stability of the trivial solution, we need to describe the regions in parameter space where this occurs. This is the content of the present section. Since the parameter space is four dimensional, it is difficult to visualize these regions. Thus we will focus on fixing the cell parameters α and τ_s and describing curves in the $\beta,\ \tau$ plane where the characteristic equation has a zero root or a pair of pure imaginary roots. In the first subsection, we define these curves. In the second subsection we describe the geometry of these curves and how this geometry changes as α and τ_s are varied.

4.1 Definition of the curves

When $\beta = \dfrac{1-\alpha}{2}$, the characteristic equation has a simple zero root (from $\Delta_0(0) = 0$) for any n, while when n is an even number, the characteristic equation has another simple zero

root (from $\Delta_{\frac{n}{2}}(0) = 0$) when $\beta = \dfrac{\alpha - 1}{2}$. When $\beta = \dfrac{1-\alpha}{2\cos\frac{2\pi j}{n}}$, $(j = 1, 2, \cdots, [\frac{n-1}{2}])$, the characteristic equation has a double zero root except when $n = 2m$, with m being an even integer, and $j = \frac{n}{4}$ (see $\Delta_{\frac{n}{4}}(\lambda)$ in eq. (16)). In this case, the characteristic equation has a double zero root when $\alpha = 1$ for any value of β (from $\Delta_{\frac{n}{4}}(0) = 1 - \alpha$).

The characteristic equation has a simple pair of pure imaginary roots $\pm i\,\omega$ when $\Delta_0(\pm i\,\omega) = 0$, i.e. when $\omega, \alpha, \beta, \tau_s, \tau$ satisfy

$$\begin{aligned} 1 - \alpha\,\cos(\omega\tau_s) &= 2\,\beta\,\cos(\omega\,\tau)\,, \\ \omega + \alpha\,\sin(\omega\tau_s) &= -2\,\beta\,\sin(\omega\,\tau)\,. \end{aligned} \tag{28}$$

For fixed α and τ_s this occurs along the curves $(\beta^{\pm}_{H0}(\omega), \tau^{\pm}_{H0k}(\omega))$ in β, τ plane where ω acts as a parameter. Define

$$\mathcal{T}_l(\omega) = \frac{1}{\omega}\left\{\mathrm{Arctan}\left[\frac{-\omega - \alpha\sin(\omega\tau_s)}{1 - \alpha\cos(\omega\tau_s)}\right] + l\pi\right\}. \tag{29}$$

Then these curves are given by

$$\beta^{\pm}_{H0}(\omega) = \pm\frac{1}{2}\sqrt{1 + \alpha^2 + \omega^2 + 2\alpha\omega\sin(\omega\tau_s) - 2\alpha\cos(\omega\tau_s)}\,, \tag{30}$$

$$\tau^{+}_{H0k}(\omega) = \begin{cases} \mathcal{T}_{2k}, & 1 - \alpha\cos(\omega\tau_s) > 0 \\ \mathcal{T}_{2k+1}, & 1 - \alpha\cos(\omega\tau_s) < 0 \end{cases}, \tag{31}$$

$$\tau^{-}_{H0k}(\omega) = \begin{cases} \mathcal{T}_{2k+1}, & 1 - \alpha\cos(\omega\tau_s) > 0 \\ \mathcal{T}_{2k}, & 1 - \alpha\cos(\omega\tau_s) < 0 \end{cases}. \tag{32}$$

When n is even, another simple pair of pure imaginary roots exists when $\Delta_{\frac{n}{2}}(\pm i\omega) = 0$, i.e. when

$$\begin{aligned} 1 - \alpha\,\cos(\omega\tau_s) &= -2\,\beta\,\cos(\omega\,\tau)\,, \\ \omega + \alpha\,\sin(\omega\tau_s) &= 2\,\beta\,\sin(\omega\,\tau)\,. \end{aligned} \tag{33}$$

This occurs along curves $(\beta^{\pm}_{Hh}(\omega), \tau^{\pm}_{Hhk}(\omega)) = (\beta^{\pm}_{H\frac{n}{2}}(\omega), \tau^{\pm}_{H\frac{n}{2}k}(\omega))$ given by

$$\beta^{\pm}_{Hh}(\omega) = \beta^{\pm}_{H0}(\omega)\,, \tag{34}$$

$$\tau^{+}_{Hhk}(\omega) = \begin{cases} \mathcal{T}_{2k}, & 1 - \alpha\cos(\omega\tau_s) < 0 \\ \mathcal{T}_{2k+1}, & 1 - \alpha\cos(\omega\tau_s) > 0 \end{cases}, \tag{35}$$

$$\tau^{-}_{Hhk}(\omega) = \begin{cases} \mathcal{T}_{2k+1}, & 1 - \alpha\cos(\omega\tau_s) < 0 \\ \mathcal{T}_{2k}, & 1 - \alpha\cos(\omega\tau_s) > 0 \end{cases}. \tag{36}$$

The characteristic equation has a repeated pair of pure imaginary roots $\lambda = \pm i\omega$ for parameters such that $\Delta_j(\pm i\omega) = 0,\ (j = 1,\, 2,\, \cdots,\, [\frac{n-1}{2}])$, i.e. when

$$\begin{aligned} 1 - \alpha\, \cos(\omega\tau_s) &= 2\,\beta\, \cos\frac{2\pi\, j}{n} \cos(\omega\,\tau)\,, \\ \omega + \alpha\, \sin(\omega\tau_s) &= -2\,\beta\, \cos\frac{2\pi\, j}{n} \sin(\omega\,\tau)\,. \end{aligned} \tag{37}$$

When $j \neq \frac{n}{4}$, this occurs along curves $(\beta^{\pm}_{Hj}(\omega), \tau^{\pm}_{Hjk}(\omega))$ given by

$$\beta^{\pm}_{Hj}(\omega) = \beta^{\pm}_{H0}(\omega)/|\cos(\frac{2\pi\, j}{n})|\,, \tag{38}$$

$$\tau^{+}_{Hjk}(\omega) = \begin{cases} \mathcal{T}_{2k}, & 1 - \alpha\cos(\omega\tau_s) > 0, \\ \mathcal{T}_{2k+1}, & 1 - \alpha\cos(\omega\tau_s) < 0, \end{cases} \quad j = 1, 2, \ldots [\tfrac{n-1}{4}]$$
$$\begin{cases} \mathcal{T}_{2k+1} & 1 - \alpha\cos(\omega\tau_s) > 0, \\ \mathcal{T}_{2k}, & 1 - \alpha\cos(\omega\tau_s) < 0, \end{cases} \quad j = [\tfrac{n}{4}] + 1, \ldots, [\tfrac{n-1}{2}] \tag{39}$$

$$\tau^{-}_{Hjk}(\omega) = \begin{cases} \mathcal{T}_{2k+1}, & 1 - \alpha\cos(\omega\tau_s) > 0, \\ \mathcal{T}_{2k}, & 1 - \alpha\cos(\omega\tau_s) < 0, \end{cases} \quad j = 1, 2, \ldots [\tfrac{n-1}{4}]$$
$$\begin{cases} \mathcal{T}_{2k}, & 1 - \alpha\cos(\omega\tau_s) > 0, \\ \mathcal{T}_{2k+1}, & 1 - \alpha\cos(\omega\tau_s) < 0, \end{cases} \quad j = [\tfrac{n}{4}] + 1, \ldots, [\tfrac{n-1}{2}] \tag{40}$$

When $j = \frac{n}{4}$, from $\Delta_{\frac{n}{4}}(\pm i\omega) = 0$ we have

$$1 - \alpha\cos(\omega\tau_s) = 0, \qquad \omega + \alpha\sin(\omega\tau_s) = 0\,. \tag{41}$$

Note that this occurs for $\alpha^2 = 1 + \omega^2 > 1$ and any β.

4.2 Geometry of the curves

In this subsection we describe the geometry of the curves defined in the previous subsection and how this geometry changes as α and τ_s are varied. We begin with three lemmas which give some basic limits and bounds of the curves.

Lemma 4.1

$$
\begin{aligned}
\lim_{\omega\to 0^+}\beta^{\pm}_{H0}(\omega) &= \lim_{\omega\to 0^+}\beta^{\pm}_{Hh}(\omega) = \pm\frac{|1-\alpha|}{2}\,,\ \lim_{\omega\to 0^+}\beta^{\pm}_{Hj}(\omega) = \pm\frac{|1-\alpha|}{2\,|\cos\frac{2\pi j}{n}|}\,,\\
\lim_{\omega\to 0^+}\tau^{\pm}_{H0k}(\omega) &= \lim_{\omega\to 0^+}\tau^{\pm}_{Hhk}(\omega) = \lim_{\omega\to 0^+}\tau^{\pm}_{Hjk}(\omega) = \infty,\ k>0,\ j=1,2,\ldots,[\tfrac{n-1}{2}] \qquad (42)\\
\lim_{\omega\to 0^+}\tau^{+}_{H00}(\omega) &= \lim_{\omega\to 0^+}\tau^{+}_{Hj0}(\omega) = \begin{cases} \frac{1+\alpha\tau_s}{\alpha-1} & \alpha<1\\ -\infty & \alpha=1\\ \infty & \alpha>1\end{cases},\quad j=1,2,\ldots,[\tfrac{n-1}{4}]\\
\lim_{\omega\to 0^+}\tau^{-}_{H00}(\omega) &= \lim_{\omega\to 0^+}\tau^{-}_{Hj0}(\omega) = \begin{cases} \frac{1+\alpha\tau_s}{\alpha-1} & \alpha>1\\ \infty & \alpha\le 1\end{cases},\quad j=1,2,\ldots,[\tfrac{n-1}{4}]\\
\lim_{\omega\to 0^+}\tau^{-}_{Hh0}(\omega) &= \lim_{\omega\to 0^+}\tau^{-}_{Hj0}(\omega) = \begin{cases} \frac{1+\alpha\tau_s}{\alpha-1} & \alpha<1\\ -\infty & \alpha=1\\ \infty & \alpha>1\end{cases},\quad j=[\tfrac{n}{4}]+1,\ldots,[\tfrac{n-1}{2}]\\
\lim_{\omega\to 0^+}\tau^{+}_{H00}(\omega) &= \lim_{\omega\to 0^+}\tau^{+}_{Hj0}(\omega) = \begin{cases} \frac{1+\alpha\tau_s}{\alpha-1} & \alpha>1\\ \infty & \alpha\le 1\end{cases},\quad j=[\tfrac{n}{4}]+1,\ldots,[\tfrac{n-1}{2}] \qquad (43)
\end{aligned}
$$

and

$$
\begin{aligned}
\lim_{\omega\to\infty}\beta^{\pm}_{H0}(\omega) &= \lim_{\omega\to\infty}\beta^{\pm}_{Hh}(\omega) = \pm\infty\,, \qquad \lim_{\omega\to\infty}\tau^{\pm}_{H0k}(\omega) = \lim_{\omega\to\infty}\tau^{\pm}_{Hhk}(\omega) = 0\,,\\
\lim_{\omega\to\infty}\beta^{\pm}_{Hj}(\omega) &= \pm\infty\,, \qquad \lim_{\omega\to\infty}\tau^{\pm}_{Hjk}(\omega) = 0\,, \qquad j=1,\,2,\,\cdots,\,[\tfrac{n-1}{2}],\quad j\neq\tfrac{n}{4}.
\end{aligned}
$$

Proof. The proof follows from straightforward calculations.

From these limits and the definitions of the $\tau^{\pm}_{Hjk}$ it is clear that the curves $(\beta^{+}_{Hj}(\omega),\tau^{+}_{Hj0}(\omega))$, $j=0,1,\ldots,[\frac{n-1}{4}]$ and the curves $(\beta^{-}_{Hj}(\omega),\tau^{-}_{Hj0}(\omega))$, $j=[\frac{n}{4}]+1,\ldots,[\frac{n}{2}]$ only lie in the (physically relevant) region $\tau\ge 0$ if $\alpha>1$ or $\alpha<0$ and $\tau_s>-\frac{1}{\alpha}\stackrel{def}{=}\tau^*$.

Theorem 4.2 *If $|\alpha|<1$, then*

(i) The curves $(\beta^{+}_{H0},\tau^{+}_{H0k})$ and $(\beta^{+}_{Hh},\tau^{+}_{Hhk})$ are bounded on the left by the line $\beta=\frac{1-|\alpha|}{2}$;

(ii) The curves $(\beta^{-}_{H0},\tau^{-}_{H0k})$ and $(\beta^{-}_{Hh},\tau^{-}_{Hhk})$ are bounded on the right by the line $\beta=\frac{|\alpha|-1}{2}$;

(iii) Each curve $(\beta^{+}_{Hj},\tau^{+}_{Hjk})$ $(j=1,\,2,\,\cdots,\,[\frac{n-1}{2}],\ j\neq\frac{n}{4})$ is bounded on the left by the corresponding line $\beta=\frac{1-|\alpha|}{2\,|\cos\frac{2\pi j}{n}|}$. These curves are all bounded on the left by the line $\beta=\frac{1-|\alpha|}{2\,|\cos\frac{(n-1)\pi}{n}|}$ when n is an odd number and by the line $\beta=\frac{1-|\alpha|}{2\,|\cos\frac{2\pi}{n}|}$ when n is an even number with $n\neq 4$.

(iv) Each curve $(\beta^-_{Hj}, \tau^-_{Hjk})\,(j = 1, 2, \cdots, [\frac{n-1}{2}],\ j \neq \frac{n}{4})$ *is bounded on the right by the corresponding line* $\beta = \frac{|\alpha|-1}{2\,|\cos\frac{2\pi j}{n}|}$. *These curves are all bounded on the right by the line* $\beta = \frac{|\alpha|-1}{2\,|\cos\frac{(n-1)\pi}{n}|}$ *when* n *is an odd number, and by the line* $\beta = \frac{|\alpha|-1}{2\,|\cos\frac{2\pi}{n}|}$ *when* n *is an even number with* $n \neq 4$.

Proof: The proofs of (i) and (ii) are the same as in [4, Lemma 1].

Proof of (iii). For $n = 4$, only the curves $(\beta^{\pm}_{H0}, \tau^{\pm}_{H0k})$ and $(\beta^{\pm}_{Hh}, \tau^{\pm}_{Hhk})$ exist. For any other n, clearly $\beta^+_{Hj} = \dfrac{\beta^+_{H0}}{|\cos\frac{2\pi j}{n}|} \geq \dfrac{1-|\alpha|}{2\,|\cos\frac{2\pi j}{n}|}$. For n odd, $|\cos\frac{2\pi j}{n}| \leq |\cos\frac{(n-1)\pi}{n}|$ and hence

$$\beta^+_{Hj} \geq \frac{1-|\alpha|}{2\,|\cos\frac{(n-1)\pi}{n}|} \geq \frac{1-|\alpha|}{2},\ j = 1, 2, \ldots, \frac{n-1}{2}.$$

For n even with $n \neq 4$, $|\cos\frac{2\pi j}{n}| \leq |\cos\frac{2\pi}{n}|$ and hence

$$\beta^+_{Hj} \geq \frac{1-|\alpha|}{2\,|\cos\frac{2\pi}{n}|} \geq \frac{1-|\alpha|}{2},\ j = 1, 2, \ldots, \frac{n}{2}-1,\ j \neq \frac{n}{4}.$$

The proof for (iv) is similar to that for (iii).

It follows from this theorem that for $\alpha \geq 0$ we have $\beta^+_{Hj}(\omega) \geq \beta^+_{Hj}(0) = \frac{1-\alpha}{2}$ and $\beta^-_{Hj}(\omega) \leq \beta^-_{Hj}(0) = \frac{\alpha-1}{2}$, $j = 0, 1, \ldots, [\frac{n}{2}],\ j \neq \frac{n}{4}$.

Theorem 4.3 *Let*

$$\tau_s^{(1)} = \frac{1}{(1+\sqrt{1+\frac{1}{|\alpha|}})\,|\alpha|}.$$

If $0 \leq \tau_s \leq \tau_s^{(1)}$, *then the curves of pure imaginary roots have the property that the* β^+_{Hj} *are all monotone increasing functions of* ω *and satisfy* $\beta^+_{Hj} > \dfrac{|1-\alpha|}{2|\cos\frac{2\pi j}{n}|}$ *while the* β^-_{Hj} *are all monotone decreasing functions of* ω *and satisfy* $\beta^-_{Hj} < -\dfrac{|1-\alpha|}{2|\cos\frac{2\pi j}{n}|}$, *for* $j = 0, 1, \cdots, [\frac{n}{2}]$, $j \neq \frac{n}{4}$ *and* $\omega > 0$. *When* $\alpha < 0$, *the converse is also true.*

Proof: The proof for the case $j = 0$ can be found in [2, Lemma 2] or [23, Lemma 1]. Note that when n is even $\beta_{H\frac{n}{2}}$ is what we call β_{Hh}. Now for $j = 1, 2, \ldots, [\frac{n}{2}]$, $j \neq \frac{n}{4}$ we have

$$\begin{aligned} \beta^{\pm}_{Hj} &= \frac{\beta^{\pm}_{H0}}{|\cos\frac{2\pi j}{n}|}, \\ \frac{d\beta^{\pm}_{Hj}}{d\omega} &= \frac{1}{|\cos\frac{2\pi j}{n}|}\frac{d\beta^{\pm}_{H0}}{d\omega}. \end{aligned} \tag{44}$$

Thus the results for these values of j follow directly from the result for $j = 0$.

It follows from this Theorem, the limits of Lemma 4.1 and the definitions that for $0 \leq \tau_s \leq \tau_s^{(1)}$ the various curves of pure imaginary roots never intersect themselves, each other, or the lines, $\beta = \pm\frac{\alpha-1}{2|\cos(\frac{2\pi j}{n})|}$, where there are zero roots. For $\tau_s > \tau_s^{(1)}$, various types of intersections can occur. The following two theorems describe two of these.

Theorem 4.4 *For $j = 1, 2, \ldots, [\frac{n}{2}]$, let $\omega^{(2j)}$ and $\tau_s^{(2j)}$ be the smallest positive numbers satisfying the equations*

$$\omega + \alpha\,(1+\tau_s)\sin(\omega\tau_s) + \alpha\omega\tau_s\cos(\omega\tau_s) = 0 \tag{45}$$

$$1 + \alpha^2 + \omega^2 + 2\alpha\omega\sin(\omega\tau_s) - 2\alpha\cos(\omega\tau_s) = (1-\alpha)^2\,|\cos\frac{2\pi j}{n}|^2. \tag{46}$$

(i) When $\tau_s = \tau_s^{(2j)}$, the minimum value of $\beta_{Hj}^+(\omega)$ is $\beta_{Hj}^+(\omega^{(2j)}) = \frac{\alpha-1}{2}$, and the maximum value of $\beta_{Hj}^-(\omega)$ is $\beta_{Hj}^-(\omega^{(2j)}) = \frac{1-\alpha}{2}$.

(ii) For each j, $\tau_s^{(2j)}$ and $\omega^{(2j)}$ exist only if $\alpha > 1$ or if $\alpha < \dfrac{|\cos\frac{2\pi j}{n}| - 1}{|\cos\frac{2\pi j}{n}| + 1}$. They exist for every j if $\alpha < \dfrac{|\cos\frac{2\pi j^*}{n}| - 1}{|\cos\frac{2\pi j^*}{n}| + 1} \stackrel{def}{=} \alpha^*$ where $j^* = [\frac{n+1}{4}]$ when n is odd and $j^* = [\frac{n-1}{4}]$ when n is even.

Proof: (i) From the definitions of the $\beta_{Hj}^{\pm}$ it is clear that, for any fixed τ_s, a solution ω of (45) corresponds to a value of ω where $\frac{d\beta_{Hj}^{\pm}}{d\omega} = 0$ for $j = 1, 2, \ldots, [\frac{n}{2}]$. From Theorem 4.3 the smallest positive such ω must correspond to a minimum of β_{Hj}^+ and a maximum of β_{Hj}^-. Similarly a solution ω of (46) corresponds to a value of ω where $\beta_{Hj}^{\pm} = \pm\frac{\alpha-1}{2}$. It is clear, then, that simultaneous solving of these two equations for ω and τ_s yields the result.

(ii) When $|\alpha| < 1$, we know from Theorem 4.2 that $\beta_{Hj}^{+min} > \dfrac{1-|\alpha|}{2|\cos\frac{2\pi j}{n}|} > \dfrac{1-|\alpha|}{2}$. When $0 \leq \alpha \leq 1$, $\beta_{Hj}^{+min} > \frac{1}{2}(1-\alpha)$, so it is impossible for (46) to be satisfied for any $\omega > 0$. When $-1 \leq \alpha < 0$, from $\dfrac{1-|\alpha|}{2|\cos\frac{2\pi j}{n}|} = \dfrac{1+\alpha}{2|\cos\frac{2\pi j}{n}|} \leq \dfrac{1-\alpha}{2}$, we can obtain the condition $\alpha < \dfrac{|\cos\frac{2\pi j}{n}| - 1}{|\cos\frac{2\pi j}{n}| + 1}$. Since the function $h(x) = \dfrac{x-1}{x+1}$ is an increasing function and $h < 0$ when $x = |\cos\frac{2\pi j}{n}|$, we can find the common condition described in the statement of the theorem since the minimum value of x occurs when $j = j^*$.

Theorem 4.5 *Let α be fixed, if $|\alpha| < 1$ then $\beta_{Hj}^{\pm} \neq 0\,,\ (j = 0,\, 1,\, \cdots,\, [\frac{n}{2}],\, j \neq \frac{n}{4})$ for any $\tau_s \geq 0$ and any $\omega > 0$. If $|\alpha| > 1$, there exists a countable infinity of values of τ_s for which $\beta_{Hj}^{\pm}(\omega) = 0$ for some $\omega > 0$.*

Proof: Setting $\beta = 0$ in eqs. (28), (33) and (37), we have

$$\alpha \cos(\omega\tau_s) = 1, \qquad \alpha \sin(\omega\tau_s) = -\omega\,, \tag{47}$$

then $\alpha^2 = 1 + \omega^2 \geq 1$.

From eq. (47), we obtain

$$\tau_s = \begin{cases} \dfrac{1}{\sqrt{\alpha^2 - 1}}[\text{Arccos}\,\dfrac{1}{\alpha} + 2\,n\,\pi], & \text{if } \alpha < -1 \\ \dfrac{1}{\sqrt{\alpha^2 - 1}}[-\ \text{Arccos}\,\dfrac{1}{\alpha} + (2\,n + 2)\,\pi], & \text{if } \alpha > 1 \end{cases} \tag{48}$$

and the result follows.

Since the trivial solution is unstable for $\alpha > 1$ we focus on the case $\alpha < -1$ and denote by $\tau_s^{(3)}$ the minimum value of τ_s for which $\beta_{Hj}^{\pm} = 0$, that is, $\tau_s^{(3)} = \frac{1}{\sqrt{\alpha^2-1}}\,\text{Arccos}\,\frac{1}{\alpha}$.

For use in the next section, we now summarize the transitions and when they occur.

- At the transition point $\tau_s^{(1)}$ the curves of pure imaginary roots may become non-monotone.

- At the transition point $\tau_s^{*} = -\frac{1}{\alpha}$ the curves $(\beta_{Hj}^{+}(\omega), \tau_{Hj0}^{+}(\omega)),\ j = 0, 1, \ldots, [\frac{n-1}{4}]$ and $(\beta_{Hj}^{-}(\omega), \tau_{Hj0}^{-}(\omega)),\ j = [\frac{n}{4}] + 1, \ldots, [\frac{n}{2}]$ enter the region $\tau \geq 0$.

- At the transition point $\tau_s^{(2j)}$ the minimum value of β_{Hj}^{+} crosses the line $\beta = \frac{1-\alpha}{2}$ and the maximum value of β_{Hj}^{-} crosses the line $\beta = \frac{\alpha-1}{2}$.

- At the transition point $\tau_s^{(3)}$ the curves $(\beta_{H0}^{\pm},\, \tau_{H0k}^{\pm}),\ (\beta_{Hh}^{\pm},\, \tau_{Hhk}^{\pm})$ and $(\beta_{Hj}^{\pm},\, \tau_{Hjk}^{\pm})$ touch the τ axis for the first time.

- When $0 \leq \alpha < 1$ only the transition at $\tau_s^{(1)}$ occurs. When $\alpha < 0$, all four types of transitions may occur, depending on the value of α. Using similar arguments to those

in [4, Lemma 5], it may be shown that the relative ordering of the transition points is

$$\tau_s^{(1)} < \tau_s^{(2\,j)} < \tau_s^{(3)} \quad \text{and} \quad \tau_s^{(1)} < \tau_s^{*} < \tau_s^{(3)}$$

Remark 4.1 *For the system (1) the transition points* $\tau_s^{(1)}$, $\tau_s^{(3)}$ *and* τ_s^{*} *are the same as those in [4], and the transition points* $\tau_s^{(2\,j)}$, $(j = 1, 2, \cdots, [\frac{n-1}{2}], j \neq \frac{n}{4})$ *are the generalizations of the transition point* $\tau_s^{(2)}$ *in [4].*

5 Full Stability Region

The stability regions with n odd are similar to that for $n = 3$ which was discussed in [4], we thus focus on the stability regions with n even.

Consider the cases $n = 2, 4$. The characteristic equations are

$$\begin{aligned} \det \mathcal{M}_4(0,\, \lambda) &= (\lambda + 1 - \alpha\, e^{-\lambda\tau_s} - 2\,\beta\, e^{-\lambda\tau})\,(\lambda + 1 - \alpha\, e^{-\lambda\tau_s} + 2\,\beta\, e^{-\lambda\tau})\,(\lambda + 1 - \alpha\, e^{-\lambda\tau_s})^2 \\ &= [\det \mathcal{M}_2(0,\, \lambda)](\lambda + 1 - \alpha\, e^{-\lambda\tau_s})^2. \end{aligned} \tag{49}$$

Thus the stability region in the β, τ plane will the same for both cases. The lines of simple zero roots are $\beta = \pm\,\dfrac{1-\alpha}{2}$, the curves of simple pairs of pure imaginary roots are $(\beta_{H0}^{\pm},\, \tau_{H0k}^{\pm})$ and $(\beta_{Hh}^{\pm},\, \tau_{Hhk}^{\pm})$. There are no repeated pairs of pure imaginary roots for either case and no double zero roots for $n = 2$ or for $n = 4$ with $\alpha \neq 1$. It follows that there are no $\tau_s^{(2j)}$ transitions. A detailed analysis follows.

I. $\alpha > 1$: There is no stability region.

II. $\alpha = 1$: The trivial solution is unstable if $\beta \neq 0$. If $\beta = 0$ the stability is not determined by the linearization.

III. $0 \leq \alpha < 1$: (See Figure 2)

The stability region is the strip bounded by the lines $\beta = \frac{1-\alpha}{2}$ and $\beta = \frac{\alpha-1}{2}$.

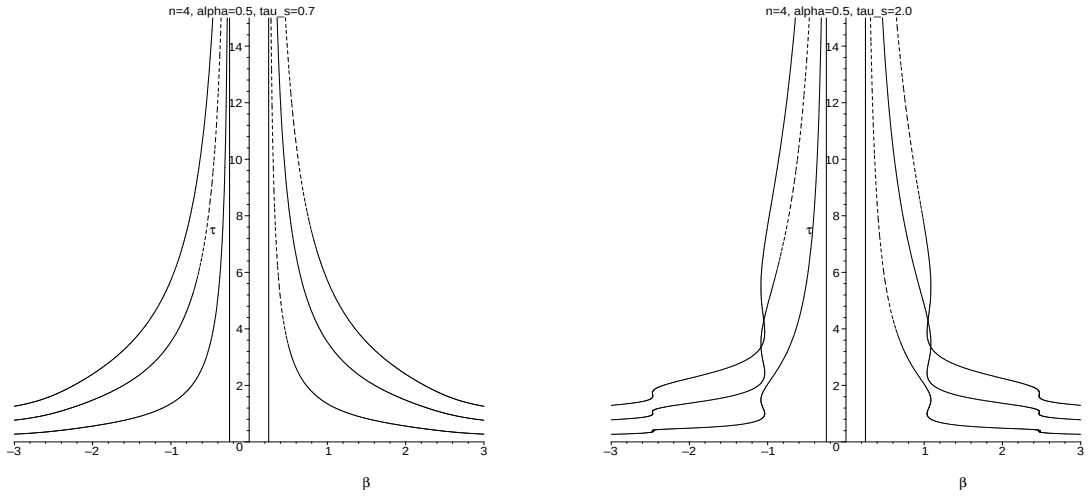

(a) $0 \le \tau_s < \tau_s^{(1)}$ (b) $\tau_s > \tau_s^{(1)}$

Figure 2: Region of local stability of the trivial solution of eq. (1) with $n = 2, 4$, $0 \le \alpha < 1$ and other parameter values as indicated.

IV. $-1 \le \alpha < 0$: (See Figure 3)

(a) $0 \le \tau_s < \tau_s^{(1)}$. The stability region is the strip bounded by the lines $\beta = \frac{1-\alpha}{2}$ and $\beta = \frac{\alpha-1}{2}$.

(b) $\tau_s^{(1)} < \tau_s < \tau_s^*$. Let ω^{int} be such that $\beta_{H0}^-(\omega^{int}) = -\beta_{Hh}^+(\omega^{int}) = \frac{\alpha-1}{2}$ and define $\tau^{int} = \tau_{H00}^-(\omega^{int}) = \tau_{Hh0}^+(\omega^{int})$. The stability region is the union of the region

$$\frac{\alpha-1}{2} < \beta < \frac{1-\alpha}{2}, \;\; 0 \le \tau \le \tau^{int};$$

and the region (with $\tau > \tau^{int}$) with boundary formed by pieces of the curves $(\beta_{H0}^+, \tau_{H0k}^+)$, $(k > 0)$, $(\beta_{Hh}^+, \tau_{Hhk}^+)$, $(k \ge 0)$ on the right, and pieces of the curves $(\beta_{H0}^-, \tau_{H0k}^-)$, $(k \ge 0)$, $(\beta_{Hh}^-, \tau_{Hhk}^-)$, $(k > 0)$ on the left.

(c) $\tau_s > \tau_s^*$. The right boundary of the stability region is made up of pieces of the line $\beta = \dfrac{1-\alpha}{2}$ and pieces of the curves $(\beta_{H0}^+, \tau_{H0k}^+)$, $(\beta_{Hh}^+, \tau_{Hhk}^+)$, $(k \ge 0)$. Symmetrically, the left boundary is made up of pieces of the line $\beta = \dfrac{\alpha-1}{2}$ and pieces of the curves $(\beta_{H0}^-, \tau_{H0k}^-)$, $(\beta_{Hh}^-, \tau_{Hhk}^-)$, $(k \ge 0)$; The right/left boundary may include the multiple

parts of $(\beta_{Hh}^{+}, \tau_{Hh0}^{+})/\ (\beta_{H0}^{-}, \tau_{H00}^{-})$.

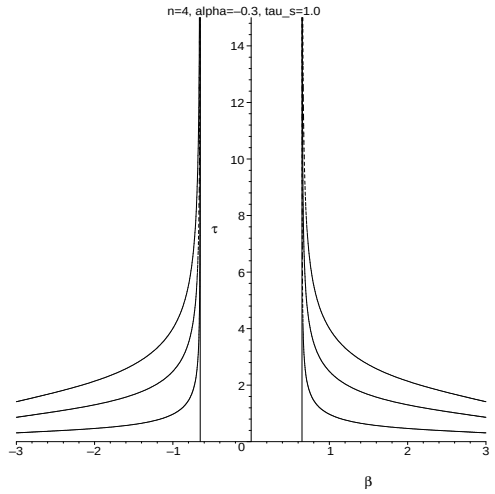

(a) $0 \leq \tau_s < \tau_s^{(1)}$

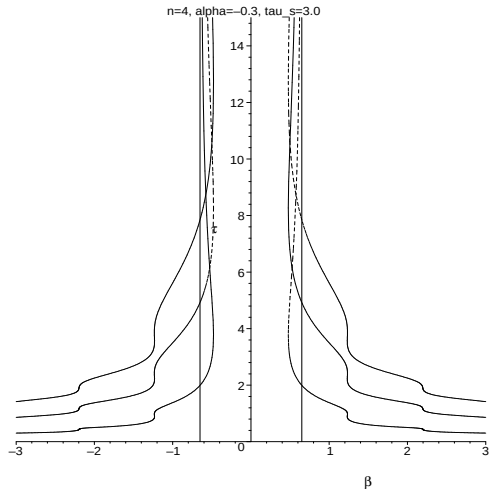

(b) $\tau_s^{(1)} < \tau_s < \tau_s^{*}$

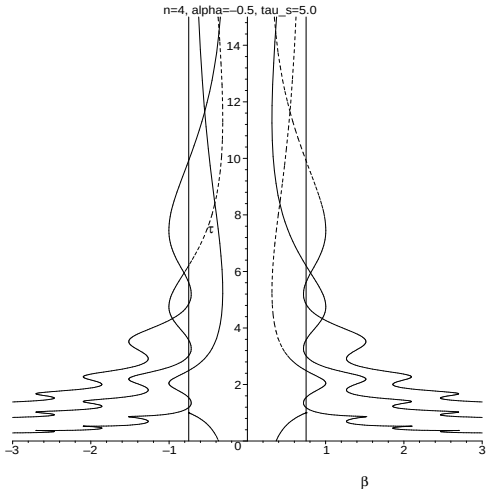

(c) $\tau_s > \tau_s^{*}$

Figure 3: Region of local stability of the trivial solution of eq. (1) with $n = 2, 4$, $-1 \leq \alpha < 0$ and other parameter values as indicated.

V. $\alpha < -1$: (See Figure 4)

(a) $0 \leq \tau_s < \tau_s^{(1)}$. Same as case IV(a).

(b) $\tau_s^{(1)} \leq \tau_s < \tau_s^{*}$. Same as case IV(b).

(c) $\tau_s^* < \tau_s < \tau_s^{(3)}$. Same as case IV(c).

(d) $\tau_s > \tau_s^{(3)}$. There is no stability region.

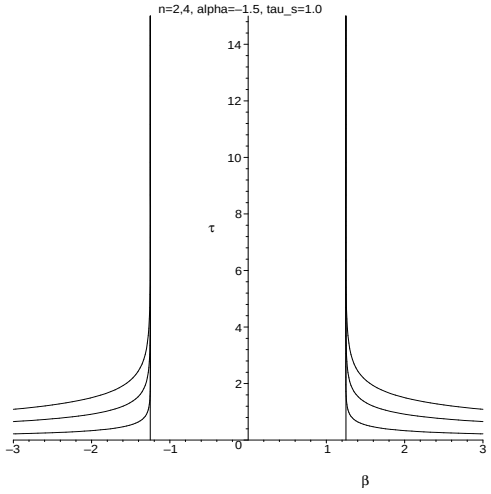

(a) $0 \leq \tau_s < \tau_s^{(1)}$

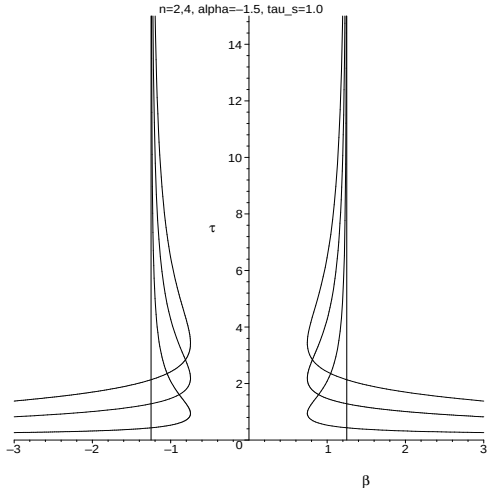

(b) $\tau_s^{(1)} < \tau_s < \tau_s^*$

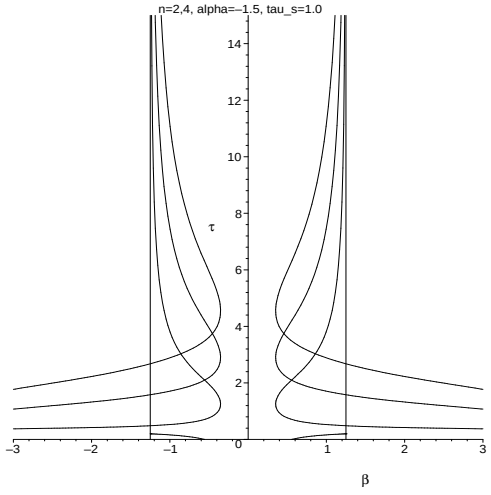

(c) $\tau_s^* < \tau_s < \tau_s^{(3)}$

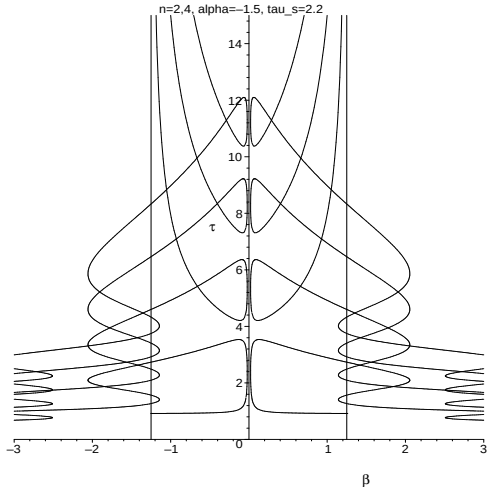

(d) $\tau_s > \tau_s^{(3)}$

Figure 4: Region of local stability of the trivial solution of eq. (1) with $n = 2, 4$, $\alpha < -1$ and other parameter values as indicated.

Now consider the case $n = 6$. The lines of simple zero roots and curves of simple pairs of pure imaginary roots are the same as in the cases $n = 2, 4$. Since $|\cos(\frac{2\pi j}{n})| = \frac{1}{2},\ j = 1, 2,$

the lines of double zero roots are $\beta = \pm(1-\alpha)$, while the curves of repeated pairs of pure imaginary roots are $(\beta_{Hj}^{\pm},\, \tau_{Hjk}^{\pm})$, $(j = 1, 2)$. The transition at $\tau^{(21)} = \tau^{(22)} = \tau^{(2)}$ occurs if $\alpha > 1$ or $\alpha < -\frac{1}{3}$, (as for the $n = 3$ case). The descriptions of the stability regions for $\alpha > 1$, $\alpha = 1$ and $0 \leq \alpha < 1$ are the same as for $n = 2, 4$. The other subcases are different due to the transition at $\tau_s^{(2)}$.

VI. $-\frac{1}{3} \leq \alpha < 0$: (See Figure 5)

(a) $0 \leq \tau_s < \tau_s^{(1)}$. Same as case IV(a).

(b) $\tau_s^{(1)} < \tau_s < \tau_s^{*}$. Same as case IV(b).

(c) $\tau_s > \tau_s^{*}$. Same as case IV(c).

VII. $-1 \leq \alpha < -\frac{1}{3}$: (See Figure 6)

(a) $0 \leq \tau_s < \tau_s^{(1)}$. Same as case IV(a).

(b) $\tau_s^{(1)} < \tau_s < \tau_s^{*}$. Same as case IV(b).

(c) $\tau_s^{*} < \tau_s < \tau_s^{(2)}$. Same as case IV(c).

(d) $\tau_s > \tau_s^{(2)}$. Same as case IV(c). See note and conjecture below.

VIII. $\alpha < -1$: (See Figure 7)

(a) $0 \leq \tau_s < \tau_s^{(1)}$. Same as case IV(a).

(b) $\tau_s^{(1)} \leq \tau_s < \tau_s^{*}$. Same as case IV(b).

(c) $\tau_s^{*} < \tau_s < \tau_s^{(2)}$. Same as case IV(c).

(d) $\tau_s^{(2)} < \tau_s < \tau_s^{(3)}$. Same as case VII(d).

(e) $\tau_s > \tau_s^{(3)}$. There is no stability region.

Remark 5.1 *In subcases VII and VIII, we have assumed that $\tau_s^{*} < \tau_s^{(2)}$. If the order is reversed then the curves $(\beta_{Hh}^{+}, \tau_{Hh0}^{+})$ and $(\beta_{Hh}^{-}, \tau_{H00}^{-})$ will become part of the stability boundary after the curves $(\beta_{Hj}^{+}, \tau_{Hjk}^{+})$. We have observed both orderings for $\alpha < -1$.*

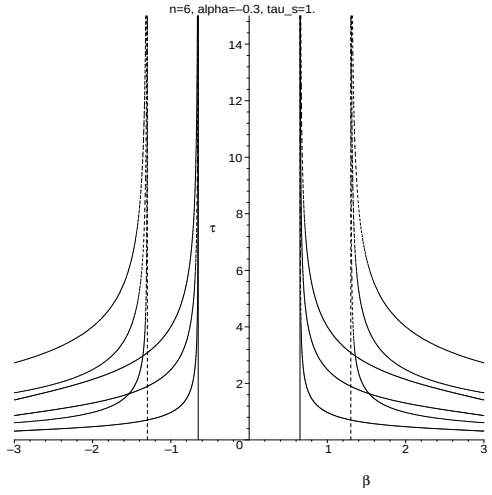

(a) $0 \leq \tau_s < \tau_s^{(1)}$

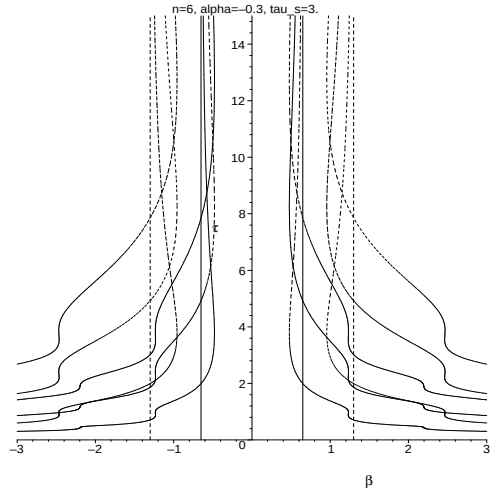

(b) $\tau_s^{(1)} < \tau_s < \tau_s^*$

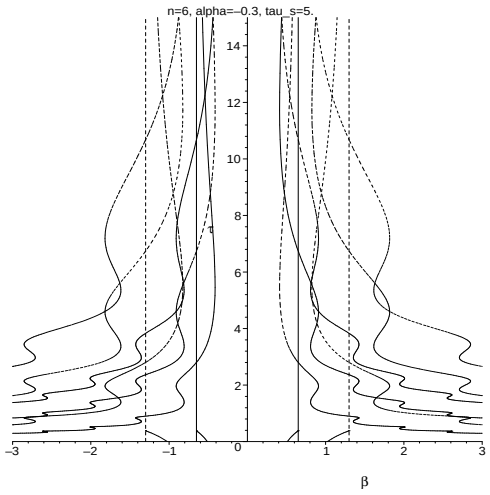

(c) $\tau_s > \tau_s^*$

Figure 5: Region of local stability of the trivial solution of eq. (1) with $n = 6$, $-\frac{1}{3} \leq \alpha < 0$ and other parameter values as indicated.

Note that in Figure 6 and in Figure 7 (a),(b),(c), the curves $(\beta_{Hj}^{\pm}, \tau_{Hjk}^{\pm}),\ j = 1, 2$ always lie outside of the curves $(\beta_{H0}^{\pm}, \tau_{H0k}^{\pm})$ and $(\beta_{Hh}^{\pm}, \tau_{Hhk}^{\pm})$. Thus only the curves $(\beta_{H0}^{\pm}, \tau_{H0k}^{\pm})$ and $(\beta_{Hh}^{\pm}, \tau_{Hhk}^{\pm})$ can form part of the boundary of the region of stability of the trivial solution and the stability region is essentially the same as in the case $n = 2, 4$. This leads us to the

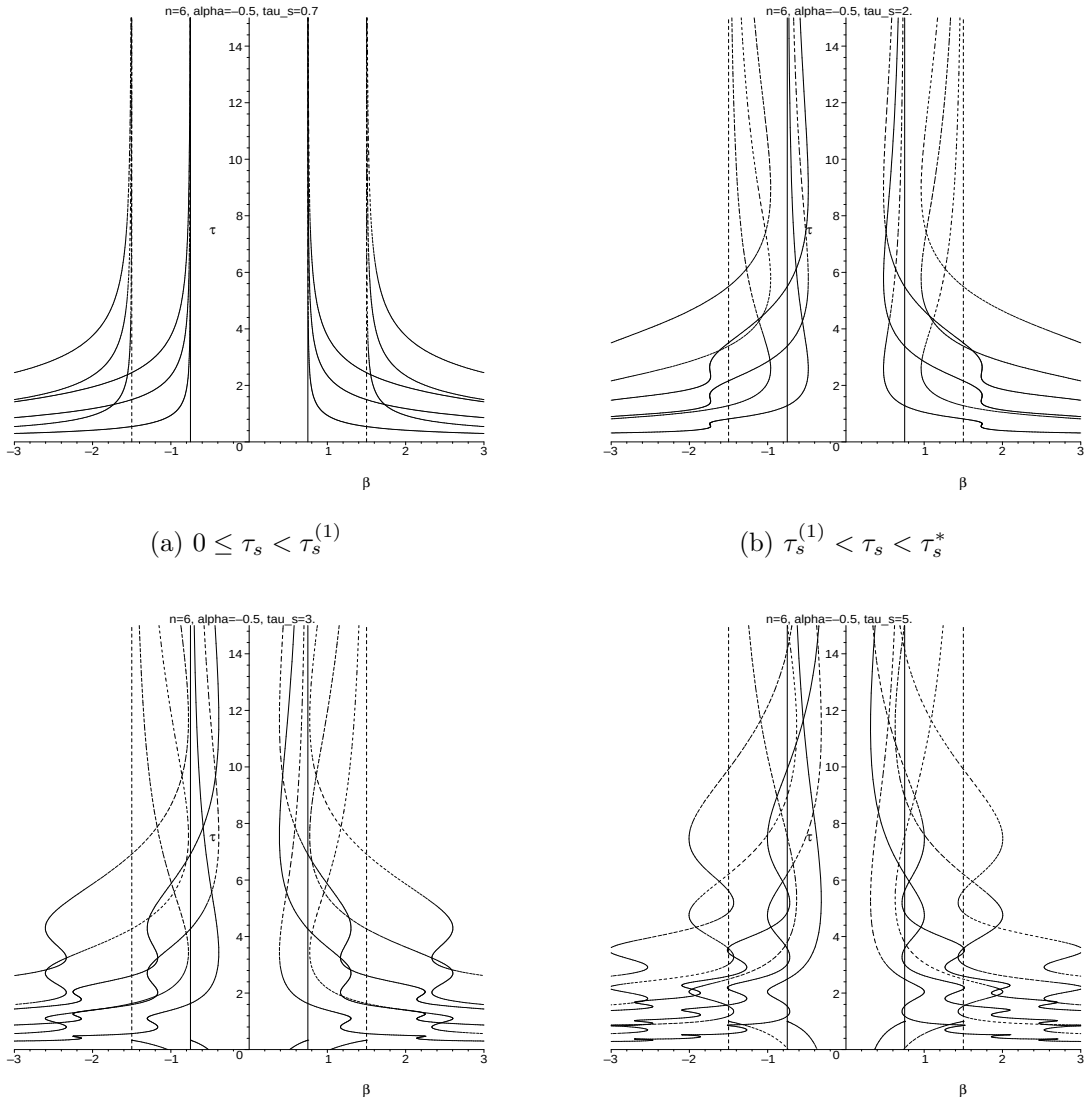

(a) $0 \leq \tau_s < \tau_s^{(1)}$

(b) $\tau_s^{(1)} < \tau_s < \tau_s^*$

(c) $\tau_s^* < \tau_s < \tau_s^{(2)}$

(d) $\tau_s > \tau_s^{(2)}$

Figure 6: Region of local stability of the trivial solution of eq. (1) with $n = 6$, $-1 \leq \alpha \leq -\frac{1}{3}$ and other parameter values as indicated.

following conjecture.

Conjecture 5.1 *Let $\alpha < \alpha^*$ be fixed and let $n = 2m,\ m = 1, 2, \ldots$. There exists $\bar{\tau}_s$ such that, when $\tau_s < \bar{\tau}_s$ for each $k = 0, 1, ..$ the part of the curve $(\beta_{Hj}^{\pm}(\omega), \tau_{Hjk}^{\pm}(\omega)),\ j = 1, 2, ...[\frac{n-1}{4}]$ with $\tau \geq 0$ lies entirely to the right (left) of the corresponding curve $(\beta_{H0}^{\pm}, \tau_{H0k}^{\pm})$. For each*

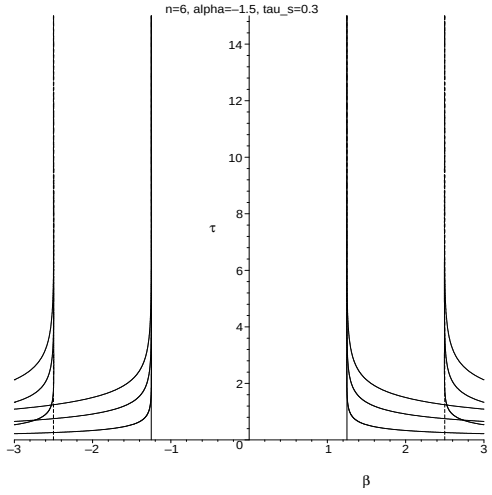

(a) $0 \leq \tau_s < \tau_s^{(1)}$

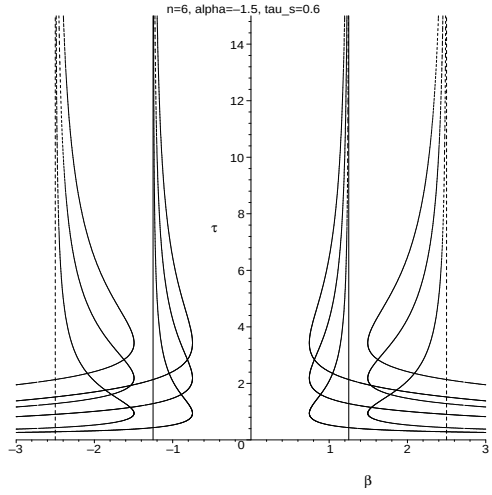

(b) $\tau_s^{(1)} < \tau_s < \tau_s^*$

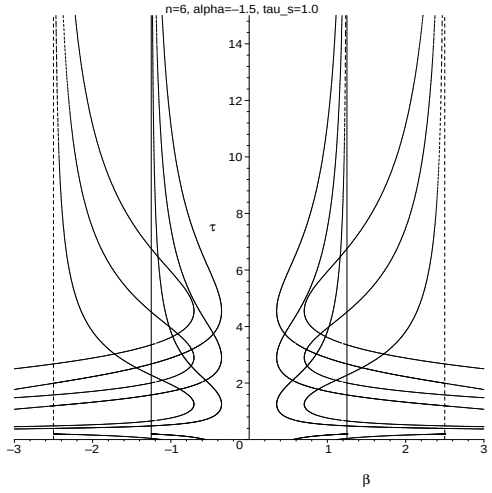

(c) $\tau_s^{(2)} < \tau_s < \tau_s^{(3)}$

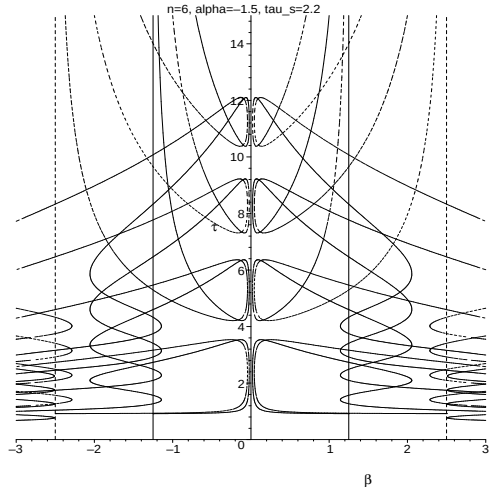

(d) $\tau_s > \tau_s^{(3)}$

Figure 7: Region of local stability of the trivial solution of eq. (1) with $n = 6$, $\alpha < -1$ and other parameter values as indicated.

$k = 0, 1, ..$ *the part of the curve* $(\beta_{Hj}^{\pm}(\omega), \tau_{Hjk}^{\pm}(\omega))$, $j = [\frac{n}{4} + 1], \ldots, m - 1$ *lies entirely to the right (left) of the corresponding curve* $(\beta_{Hh}^{\pm}, \tau_{Hhk}^{\pm})$. *When* $\alpha < -1$, $\bar{\tau}_s = \tau_s^{(3)}$.

For comparison, we end this section by showing (Figure 8) the stability region for $n = 3$ in the case corresponding to Case VII.

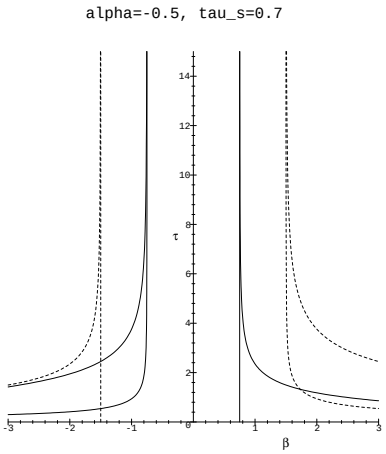

(a) $0 \leq \tau_s < \tau_s^{(1)}$

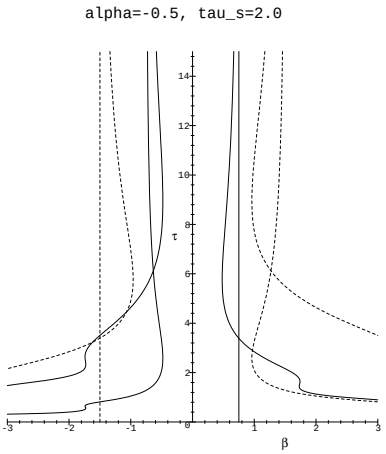

(b) $\tau_s^{(1)} < \tau_s < \tau_s^*$

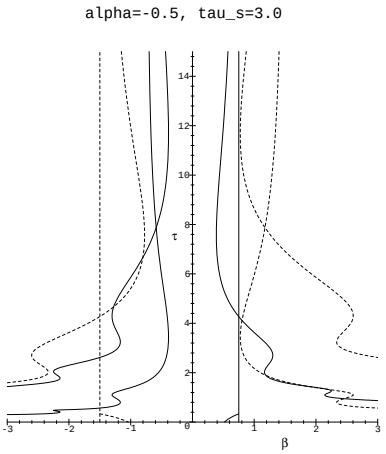

(c) $\tau_s^* < \tau_s < \tau_s^{(2)}$

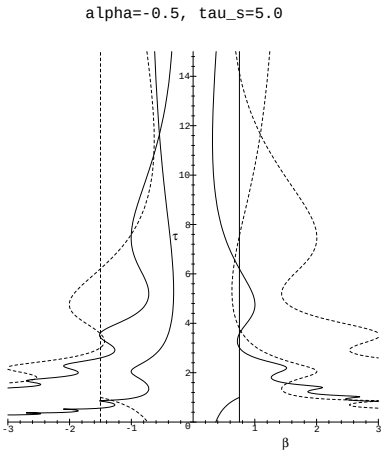

(d) $\tau_s > \tau_s^{(2)}$

Figure 8: Region of local stability of the trivial solution of eq. (1) with $n = 3$, $-1 < \alpha < -\frac{1}{3}$ and other parameter values as indicated. Compare with Figure 6.

6 Global Stability and Synchronization

In this section we use Lyapunov functionals to establish some global stability results for the trivial solution, and discuss conditions for the synchronization of solutions.

Theorem 6.1 *If $|\alpha|+2|\beta|<1$, then the trivial solution of eq. (1) is globally asymptotically stable.*

Proof: Let

$$V(x)(t)=\sum_{j=1}^{n}x_j^2(t)+|\alpha|\sum_{j=1}^{n}\int_{t-\tau_s}^{t}f^2(x_j(v))dv+|\beta|\sum_{j=1}^{n}[\int_{t-\tau}^{t}g^2(x_{j-1}(v))dv+\int_{t-\tau}^{t}g^2(x_{j+1}(v))dv]$$

then

$$\begin{aligned}
\frac{dV}{dt} &= 2\sum_{j=1}^{n}x_j(t)\dot{x}_j(t)+|\alpha|\sum_{j=1}^{n}[f^2(x_j(t))-f^2(x_j(t-\tau_s))]\\
&\quad+|\beta|\sum_{j=1}^{n}[g^2(x_{j-1}(t))-g^2(x_{j-1}(t-\tau))+g^2(x_{j+1}(t))-g^2(x_{j+1}(t-\tau))]\\
&\qquad\qquad(\text{ Note: } x_0\equiv x_n,\ x_{n+1}\equiv x_1)\\
&= 2\sum_{j=1}^{n}x_j\{-x_j+\alpha f(x_j(t-\tau_s))+\beta[g(x_{j-1}(t-\tau))+g(x_{j+1}(t-\tau))]\}\\
&\quad+|\alpha|\sum_{j=1}^{n}[f^2(x_j(t))-f^2(x_j(t-\tau_s))]\\
&\quad+|\beta|\sum_{j=1}^{n}[g^2(x_{j-1}(t))-g^2(x_{j-1}(t-\tau))+g^2(x_{j+1}(t))-g^2(x_{j+1}(t-\tau))]\\
&\le -2\sum_{j=1}^{n}x_j^2+|\alpha|\sum_{j=1}^{n}[x_j^2+f^2(x_j(t-\tau_s))]+|\beta|\sum_{j=1}^{n}[x_j^2+g^2(x_{j-1}(t-\tau))]\\
&\quad+|\beta|\sum_{j=1}^{n}[x_j^2+g^2(x_{j+1}(t-\tau))]+|\alpha|\sum_{j=1}^{n}[f^2(x_j(t))-f^2(x_j(t-\tau_s))]\\
&\quad+|\beta|\sum_{j=1}^{n}[g^2(x_{j-1}(t))-g^2(x_{j-1}(t-\tau))+g^2(x_{j+1}(t))-g^2(x_{j+1}(t-\tau))]\\
&\le -2\sum_{j=1}^{n}x_j^2+|\alpha|\sum_{j=1}^{n}x_j^2+2|\beta|\sum_{j=1}^{n}x_j^2+|\alpha|\sum_{j=1}^{n}f^2(x_j(t))\\
&\quad+|\beta|\sum_{j=1}^{n}[g^2(x_{j-1}(t))+g^2(x_{j+1}(t))]\,, \qquad (50)
\end{aligned}$$

Rewrite

$$f(x_j(t))=p_j(t)x_j(t)\qquad g(x_j(t))=q_j(t)x_j(t)\,, \qquad (51)$$

where

$$p_j(t) = \int_0^1 f'(v\, x_j(t))dv \qquad q_j(t) = \int_0^1 g'(v\, x_j(t))dv\,. \tag{52}$$

From the conditions (C1)–(C4) on f and g, there exist $p^*,\, q^* \in (0,\, 1]$ such that $p_j(t) \leq p^*,\ q_j(t) \leq q^*,\ (j = 1,\, 2,\, \cdots,\, n)$. Thus we have

$$\begin{aligned}
\frac{dV}{dt} &\leq -2\sum_{j=1}^{n} x_j^2 + (|\alpha| + 2|\beta|)\sum_{j=1}^{n} x_j^2 + |\alpha| p^* \sum_{j=1}^{n} x_j^2 + 2|\beta| q^* \sum_{j=1}^{n} x_j^2 \\
&\leq (-2 + |\alpha| + 2|\beta| + |\alpha| + 2|\beta|)\sum_{j=1}^{n} x_j^2 \\
&= -2[1 - (|\alpha| + 2|\beta|)]\sum_{j=1}^{n} x_j^2,
\end{aligned} \tag{53}$$

and for $|\alpha| + 2|\beta| < 1$, the trivial solution of eq. (1) is globally asymptotically stable.

We note that the condition in Theorem 6.1 is the same as that in [4] for $n = 3$. When $\alpha > 0$ and n is even, this theorem shows that the region of local stability of the trivial solution obtained in the previous section (see case III and Figure 2) is in fact the region of global stability. In other cases this region of global stability corresponds to the region of delay independent local stability (see Figures 5,6,8). For $\alpha < 0$, to get a weaker condition on α and β which guarantees global stability, we need to have conditions including the delay. Using the conditions given in [24] (for a network of arbitrary size and connection structure), we have the following result.

Theorem 6.2 *If $\alpha < 0$, $|\beta| < \frac{1-\alpha}{2}$ and $0 < \tau_s < \dfrac{1}{1 - e\,\alpha} \stackrel{def}{=} \tau_s^g$, then the trivial solution of (1) is globally asymptotically stable.*

Noting that $\tau_s^g < \tau_s^{(1)}$, we see that the region of local stability of the trivial solution, for $\alpha < 0$ and n even, obtained in the previous section is also a region of global stability for τ_s small enough. (See subcases IV(a), V(a), VI(a), VII(a) and VIII(a) and Figures 3(a)–7(a)). For n odd and $\alpha < 0$ this region of global stability corresponds to the region of τ independent local stability (see Figure 8(a)).

Following the definitions in [27], we say that a solution $x(t)$ of (1) is asymptotically synchronous if the ω-limit set of $x_t(\theta)$ is contained in the set of synchronous phase points,

given by

$$\{(\phi_1, \phi_2, \ldots, \phi_n)^T \in C; \quad \phi_1 = \phi_2 = \cdots = \phi_n\}. \tag{54}$$

If every solution of (1) is asymptotically synchronous, then the system is said to be absolutely synchronous.

For delay independent synchronization results, we believe that one cannot do better than the global stability result (the condition in Theorem 6.1.) when n is even. The reason is that the Hopf bifurcation curves corresponding to $\Delta_{\frac{n}{2}}(\lambda)$ will enter any region in the (β, τ) plane with $|\beta| > \dfrac{1-|\alpha|}{2}$ if τ_s is large enough (we can see this in the figures, it also follows from the results of Theorems 4.2 and 4.3). Since crossing these curves can lead to stable asynchronous solutions, we can not have absolute synchronization in any region with $|\beta| > \dfrac{1-|\alpha|}{2}$.

We may be able to do better when n is odd. In this case the asynchronous Hopf bifurcation curves always remain outside the region $|\beta| < \dfrac{1-|\alpha|}{2\,|\cos\frac{(n-1)\pi}{n}|}$ (when $|\alpha| < 1$). So a possible condition is $|\alpha| + 2\,|\cos\frac{(n-1)\pi}{n}||\beta| < 1$. This reduces to the condition for $n = 3$, $|\alpha| + |\beta| < 1$, given in [4] and [27].

Summarizing the above discussion, we have the following conjecture.

Conjecture 6.3 *When n is an odd number, system (1) is absolutely synchronous if $|\alpha| + 2\,|\cos\frac{(n-1)\pi}{n}||\beta| < 1$; while when n is an even number, system (1) is not absolutely synchronous if $|\alpha| + 2\,|\beta| > 1$.*

We illustrate this conjecture with some numerical simulations of the full model (1) with $f = g = \tanh$ in Figures 9 and 10. The simulations were performed with XPPAUT [7], using a 4th order Runge-Kutta solver adapted for delay differential equations.

7 Synchronized Bifurcations

In this section we consider the bifurcations which occur along the curves in parameter space where Δ_0 has a root with zero real part. Noting that the solution of (4) corresponding to

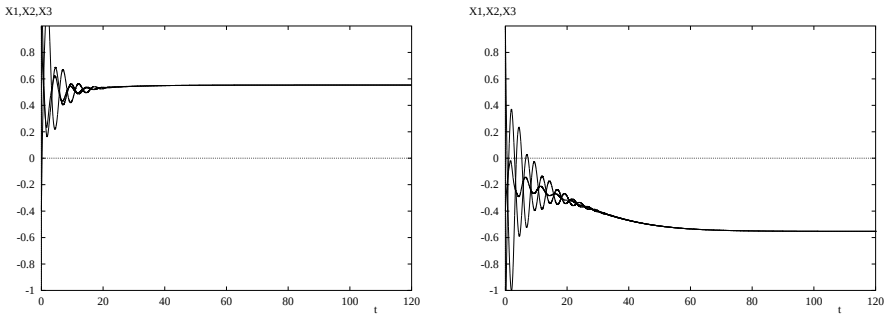

(a) Initial conditions:
$x_{10} = 1$, $x_{20} = -0.4$, $x_{30} = 1.5$

(b) Initial conditions:
$x_{10} = 1$, $x_{20} = -0.4$, $x_{30} = -1.5$

Figure 9: Numerical simulations of eq. (1) with $n = 3$ showing the co-existence of two stable synchronous equilibria for $\alpha = -0.5,\ \beta = 0.8,\ \tau_s = 2,\ \tau = 1.5$. Two different initial conditions of the form $x_j(t) = x_{j0},\ -\tau_s \leq t \leq 0$ were used. Parameter values correspond to the stability diagram of Figure 8(b).

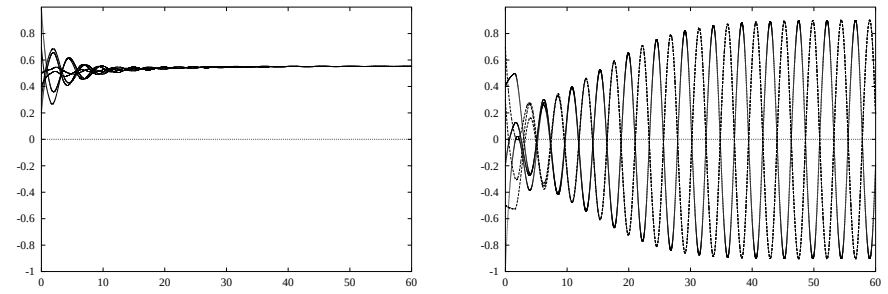

(a) Initial conditions:
$x_{10} = 1,\ x_{20} = 0.5,\ x_{30} = 0.2,$
$x_{40} = 0.7,\ x_{50} = 0.4,\ x_{60} = 0.3$

(b) Initial conditions:
$x_{10} = -1, x_{20} = -0.5, x_{30} = -0.2,$
$x_{40} = 0.7,\ x_{50} = 0.4,\ x_{60} = 0.3$

Figure 10: Numerical simulations of eq. (1) with $n = 6$ showing the co-existence of a stable synchronous equilibria with a stable asynchronous (anti-phase) limit cycle for $\alpha = -0.5,\ \beta = 0.8,\ \tau_s = 2\ \tau = 1.5$. Two different initial conditions of the form $x_j(t) = x_{j0},\ -\tau_s \leq t \leq 0$ were used. Parameter values correspond to the stability diagram of Figure 6(b).

a root λ of Δ_0 has the form $\mathbf{u}(t) = e^{\lambda t}(u, u, \ldots, u)^T$, it is clear that these correspond to bifurcations of nontrivial synchronized solutions from the trivial solution.

To begin, we verify that the characteristic equation has a simple pair of pure imaginary roots which cross the imaginary axis with nonzero speed; this means that a Hopf bifurcation occurs [14, Chapter 11]. We follow with a centre manifold analysis of the criticality of Hopf bifurcation which will determine the stability of the bifurcating periodic orbits.

Denote by $S(\lambda)$ the characteristic polynomial, i.e.

$$S(\lambda) = \det \mathcal{M}_n(0,\, \lambda) = \prod_{j=0}^{n-1}(\lambda + 1 - \alpha\, e^{-\lambda\,\tau_s} - 2\,\beta\, e^{-\lambda\,\tau}\, \cos\frac{2\pi\, j}{n}) = \prod_{j=0}^{n-1} \Delta_j(\lambda).$$

As discussed in section 4, $S(\pm i\omega) = \Delta_0(\pm i\omega) = 0$ when $\omega, \alpha, \beta, \tau_s, \tau$ satisfy eq. (28). It is easy to see that under these conditions $\Delta_j(\pm i\omega) \neq 0$ for $j \neq 0$ (cf. eq. (33) and eq. (37)). Thus we have

$$\left.\frac{\partial S}{\partial \lambda}\right|_{\lambda=i\omega} = \frac{\partial \Delta_0(i\omega)}{\partial \lambda} \prod_{j=1}^{n-1} \Delta_j(i\omega)\,, \tag{55}$$

and to check that the roots are simple, it is enough to check that $\left.\dfrac{\partial \Delta_0(i\omega)}{\partial \lambda}\right|_{\lambda=i\omega} \neq 0$. Since

$$\Delta_0(\lambda) = \lambda + 1 - \alpha\, e^{-\lambda\,\tau_s} - 2\,\beta\, e^{-\lambda\tau}, \tag{56}$$

this leads to the conditions

$$\begin{aligned} k_{11} &= 1 + \alpha\,\tau_s \cos(\omega\tau_s) + 2\beta\tau \cos(\omega\tau) \neq 0\,, \\ k_{12} &= \alpha\tau_s \sin(\omega\tau_s) + 2\beta\tau \sin(\omega\tau) \neq 0\,. \end{aligned} \tag{57}$$

Now we fix all the parameters except the delay τ and find conditions to guarantee that $Re(\left.\dfrac{d\lambda}{d\tau}\right|_{\lambda=i\omega}) \neq 0$, i.e. that the transversality condition for Hopf bifurcation is satisfied. Suppose $\lambda = \lambda(\tau)$, then from the characteristic equation $S(\lambda, \tau) = 0$ we have

$$\frac{dS}{d\tau} = \frac{\partial S}{\partial \tau} + \frac{\partial S}{\partial \lambda}\frac{d\lambda}{d\tau} = 0, \tag{58}$$

which gives

$$\frac{d\lambda}{d\tau} = -\frac{\partial S}{\partial \tau} \Big/ \frac{\partial S}{\partial \lambda}\,. \tag{59}$$

From the discussion above, it is easy to see that

$$\left.\frac{\partial S}{\partial \tau}\right|_{\lambda=i\omega} = \frac{\partial \Delta_0(i\omega)}{\partial \tau} \prod_{j=1}^{n-1} \Delta_j(i\omega)\,. \tag{60}$$

Putting this together with (55) gives

$$\left.\frac{d\lambda}{d\tau}\right|_{\lambda=i\omega} = -\left.\frac{\partial S}{\partial \tau}\right/\left.\frac{\partial S}{\partial \lambda}\right|_{\lambda=i\omega} = -\frac{\partial \Delta_0(i\omega)}{\partial \tau}\Big/\frac{\partial \Delta_0(i\omega)}{\partial \lambda}\,. \tag{61}$$

Using (56) we have

$$\mathrm{Re}\,(\left.\frac{d\lambda}{d\tau}\right|_{\lambda=i\omega}) = -\frac{2\,\beta\,\omega\,(\sin(\omega\tau) + \alpha\,\tau_s \sin(\omega\,(\tau-\tau_s)))}{k_{11}^2 + k_{12}^2}\,, \tag{62}$$

where k_{11} and k_{12} are defined in (57). It is then clear that the transversality condition is

$$\beta\,\omega\,(\sin(\omega\tau) + \alpha\,\tau_s \sin(\omega\,(\tau-\tau_s))) \neq 0\,. \tag{63}$$

We summarize the above results in the following theorem:

Theorem 7.1 *For fixed $\omega > 0, \alpha, \tau_s \geq 0$ and for β satisfying $\beta = \beta_{H0}^{\pm}$ as defined by (30), system (1) undergoes a Hopf bifurcation at $\tau = \tau_{H0k}^{\pm}$ as defined by (31)–(32) if conditions (57) and (63) hold.*

We follow the approach of [8, 13, 22, 25] in calculating the center manifold reduction. To begin, we choose a basis for the solutions of the linear DDE (4) corresponding to the simple pair of pure imaginary roots, $\pm i\omega$, of Δ_0:

$$\Phi(\theta) = (\phi_1(\theta),\, \phi_2(\theta))\,, \tag{64}$$

where

$$\phi_1 = \begin{pmatrix} 1 \\ 1 \\ \vdots \\ 1 \end{pmatrix} e^{i\omega\,\theta}, \qquad \phi_2 = \begin{pmatrix} 1 \\ 1 \\ \vdots \\ 1 \end{pmatrix} e^{-i\omega\,\theta}\,. \tag{65}$$

Then from $K =< \Phi^T, \Phi >$, we can construct the basis in the complement space

$$\Psi(\xi) = K^{-1}\,\Phi^T(\xi)\,. \tag{66}$$

It can be shown that

$$\Psi(0) = \begin{pmatrix} D_1 + i\,D_2 & D_1 + i\,D_2 & \cdots & D_1 + i\,D_2 \\ D_1 - i\,D_2 & D_1 - i\,D_2 & \cdots & D_1 - i\,D_2 \end{pmatrix}, \tag{67}$$

where

$$\begin{aligned} D_1 &= \frac{d_1}{n\,d}, \qquad D_2 = \frac{d_2}{n\,d}, \\ d_1 &= 1 + \tau + (\tau_s - \tau)\alpha\cos\omega\tau_s\,, \quad d_2 = -\,\omega\,\tau + (\tau_s - \tau)\alpha\sin\omega\tau_s\,, \\ d &= 2\,\alpha(\tau_s - \tau)[\,(1+\tau)\,\cos\omega\tau_s - \omega\,\tau\,\sin\omega\tau_s] + \alpha^2\,(\tau_s - \tau)^2 + (1+\tau)^2 + \omega^2\,\tau^2 \\ &= (1 + \tau - \alpha\,(\tau - \tau_s)\,\cos\omega\tau_s)^2 + (\alpha(\tau - \tau_s)\,\sin\omega\tau_s + \omega\tau)^2\,. \end{aligned} \tag{68}$$

Then the "form" of the center manifold is

$$\dot{\mathbf{z}}(t) = B\,\mathbf{z}(t) + \Psi(0)\mathbf{f}(\Phi(\theta)\,\mathbf{z}(t)) \tag{69}$$

where

$$B = \begin{pmatrix} i\,\omega & 0 \\ 0 & -i\,\omega \end{pmatrix}, \qquad \mathbf{z} = (z,\,\bar{z})^T\,. \tag{70}$$

Since

$$\mathbf{f}(\Phi\,\mathbf{z}) = [f_1\;\,f_2\;\,\ldots\;\,f_n]^T\,(\Phi\,\mathbf{z})\,,$$

the criticality is determined by the nonlinearities f and g in system (1). Using $f = g = \tanh$, in the neighborhood of the equilibrium $(0,\,0,\,\cdots,\,0)$, the polynomial approximation of (1) up to the third order is

$$\begin{aligned} \dot{x}_i(t) &= -x_i(t) + \alpha\,x_i(t - \tau_s) + \beta[x_{i-1}(t - \tau) + x_{i+1}(t - \tau)] \\ &\quad - \frac{1}{3}[\alpha\,x_i^3(t - \tau_s) + \beta\,x_{i-1}(t - \tau) + \beta\,x_{i+1}^3(t - \tau)] \quad (i\ mod\ n)\,, \end{aligned} \tag{71}$$

then by setting $z = x + i\,y$ we obtain

$$\begin{aligned} f_j(\Phi\,\mathbf{z}) &= -\frac{1}{3}\,[\alpha\,(z\,e^{-i\omega\tau_s} + \bar{z}\,e^{i\omega\tau_s})^3 + 2\,\beta\,(z\,e^{-i\omega\tau} + \bar{z}\,e^{i\omega\tau})^3] \\ &= -\frac{8}{3}[\alpha\,(x\,\cos(\omega\tau_s) + y\,\sin(\omega\tau_s))^3 + 2\,\beta\,(x\,\cos(\omega\tau) + y\,\sin(\omega\tau))^3] \equiv f^* \\ &\qquad\qquad (j = 1,\,2,\,\ldots,\,n)\,. \end{aligned} \tag{72}$$

To determine the Hopf bifurcation, it is important to obtain the normal form first, and then determine the sign of parameter. Now the normal form of Hopf bifurcation in polar coordinates is [12]

$$\dot{r} = a\, r^3\,, \qquad \dot{\theta} = \omega + b\, r^2\,. \tag{73}$$

Since all the components in the first row of $\Psi(0)$ are the same, $(D_1 + D_2\, i)$, so are the components in $f_j(\Phi\, \mathbf{z})$. Then

$$\Psi(0)\, \mathbf{f}(\Phi \mathbf{z}) = \begin{pmatrix} \left(\dfrac{d_1}{n\, d} + \dfrac{d_2}{n\, d}\, i\right)\, n\, f^* \\ \left(\dfrac{d_1}{n\, d} - \dfrac{d_2}{n\, d}\, i\right)\, n\, f^* \end{pmatrix} = \begin{pmatrix} \left(\dfrac{d_1}{d} + \dfrac{d_2}{d}\, i\right)\, f^* \\ \left(\dfrac{d_1}{d} - \dfrac{d_2}{d}\, i\right)\, f^* \end{pmatrix}. \tag{74}$$

Therefore, using the general Maple program we have developed, we can find the cubic coefficient

$$a = -\,\frac{\alpha(\tau - \tau_s)(\omega\, \sin\omega\tau_s - \cos\omega\tau_s) + \tau\,(1+\omega^2) + 1}{(1 + \tau - \alpha\,(\tau - \tau_s)\, \cos\omega\tau_s)^2 + (\alpha(\tau - \tau_s)\, \sin\omega\tau_s + \omega\tau)^2}\,. \tag{75}$$

From the above equation, we can observe that:

(i) The criticality of the bifurcation is determined by the sign of

$$N = -\,[\,\alpha(\tau - \tau_s)(\omega\, \sin\omega\tau_s - \cos\omega\tau_s) + \tau\,(1+\omega^2) + 1\,]$$

When $N < 0$, the bifurcation is supercritical, i.e. the Hopf bifurcation yields a stable limit cycle, while if $N > 0$, the bifurcation is subcritical and the Hopf bifurcation yields an unstable limit cycle.

(ii) The bifurcation condition is the same regardless the number of neurons n.

A similar analysis can be used to show that with $f = g = \tanh$ a pitchfork bifurcation of synchronous equilibria occurs at $\beta = \frac{1-\alpha}{2}$. This bifurcation is supercritical/subcritical if

$$1 + \alpha\tau_s + \tau(1-\alpha) \gtrless 0.$$

Figure 9 shows the equilibria resulting from a supercritical pitchfork bifurcation.

From Figures 5– 8 it is clear that if $\tau_s > \tau_s^{(1)}$ then interactions of the various synchronous bifurcations can occur. This can lead to coexistence of various stable synchronous solutions. We illustrate this with numerical simulations in Figures 11 and 12.

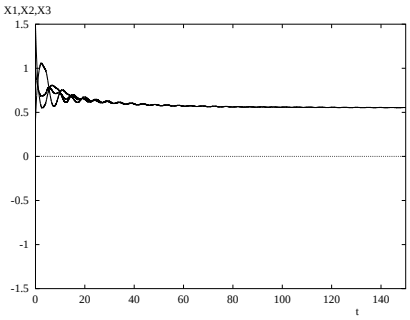

(a) Initial conditions:
$x_{10} = 1,\ x_{20} = 0.4,\ x_{30} = 1.5.$

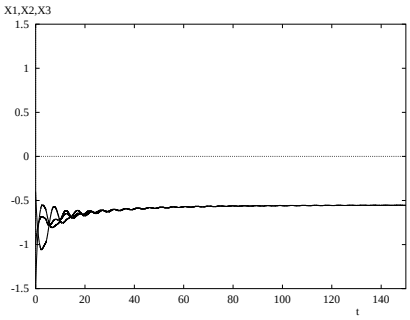

(b) Initial conditions:
$x_{10} = -1,\ x_{20} = -0.4,\ x_{30} = -1.5.$

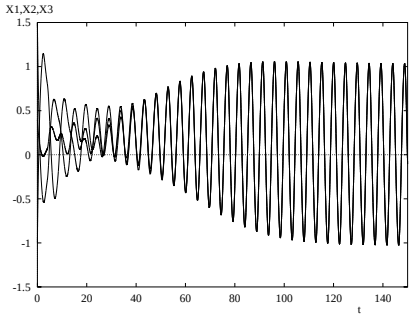

(c) Initial conditions:
$x_{10} = -1,\ x_{20} = 0.4,\ x_{30} = 1.5.$

Figure 11: Numerical simulations of the network with $n = 3$ showing the co-existence of two stable synchronous equilibria with a synchronous periodic orbit for $\alpha = -0.5,\ \beta = 0.8,\ \tau_s = 2,\ \tau = 4$. Three different initial conditions of the form $x_j(t) = x_{j0},\ -\tau_s \leq t \leq 0$ were used. Parameter values correspond to the stability diagram of Figure 8(b).

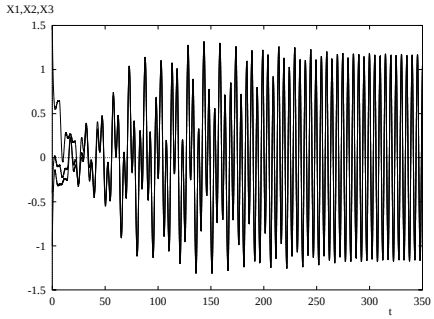

(a) Initial conditions: $x_{10} = -1,\ x_{20} = -0.4,\ x_{30} = 1.5$.

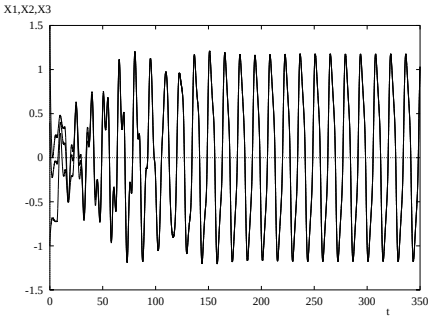

(b) Initial conditions: $x_{10} = -1,\ x_{20} = 0.4,\ x_{30} = 1.5$.

Figure 12: Numerical simulations of the network with $n = 3$ showing the co-existence of two stable synchronous periodic orbits for $\alpha = -0.5,\ \beta = -0.8,\ \tau_s = 2,\ \tau = 6.8$. Two different initial conditions of the form $x_j(t) = x_{j0},\ -\tau_s \leq t \leq 0$ were used. Parameter values correspond to the stability diagram of Figure 8(b).

8 Discussion

In this paper, we extend the local and global stability results of [4] for a ring of 3 identical elements with time delayed nearest neighbour coupling to the case of general n. We also analyze the (simple) Hopf and steady state bifurcations of synchronous solutions from the trivial solution, including a centre manifold analysis of the criticality of these bifurcations.

In particular, we have shown that certain regions where there is delay independent local stability of the trivial solution there is also global stability. We have seen that when there is an even number of elements in the ring, the region of local stability is the same as for a ring with just two elements, if the self delay, τ_s is sufficiently small. We have shown that synchronous nontrivial equilibria and limit cycles can arise via steady state and Hopf bifurcations from the trivial solution. Using the nonlinearities $f = g = \tanh$ we have shown that these nontrivial synchronous solutions can be stable and can coexist.

In order to be able to carry out our analysis, we have chosen a specific model for the elements in our ring. In general terms, each diagram of Figures 3–8 shows the stability/bifurcation of the trivial solution in terms of the coupling delay, τ, and the coupling

strength β. The sequences of diagrams in each set show how these properties change as we vary a parameter which is associated with the emergence of periodic solutions in the individual elements. We conjecture that qualitatively similar diagrams will occur if a different model for the elements was used, but the delayed, nearest neighbour coupling was retained. As evidence of this, we note the work of [3], who studied a "ring" of two elements, each element being modeled by a systems of three nonlinear ordinary differential equations capable of oscillating. They obtain a sequence of stability/bifurcation diagrams very similar to that of Figure 4 and find stable synchronous periodic orbits which bifurcate from the trivial solution.

Of further interest in this model is the existence and stability of the various asynchronous solutions which may bifurcate from the trivial solution. This paper represents some progress in this regard. Under appropriate conditions on the nonlinearities, the curves in our stability diagrams where the characteristic equation has a double zero root or a repeated pair of pure imaginary roots will correspond to equivariant steady state and equivariant Hopf bifurcations. It is clear that, when n is even, stable anti-phase solutions can exist, cf. Figure 10. Also, it has been shown in [4] that for $n = 3$ other stable asynchronous solutions may exist. We leave further pursuit of this line of research to a future paper [5].

References

[1] J. Bélair and S. A. Campbell, "Stability and bifurcations of equilibria in a multiple-delayed differential equation", *SIAM J. Appl. Math* **54**(5), 1402–1424, 1994.

[2] S.A. Campbell, "Stability and bifurcation of a simple neural network with multiple time delays", in *Differential Equations with Application to Biology*, S. Ruan, G.S.K. Wolkowicz and J. Wu eds, Fields Institute Communications Vol. 21, 65–79, AMS, 1999.

[3] S.A. Campbell, R. Edwards and P. van den Driessche "Delayed coupling between two neural network loops", *SIAM. J. Appl. Math*, in press, 2004.

[4] S.A. Campbell, I. Ncube and J. Wu, "Multistability and stable asynchronous periodic oscillations in a multiple-delayed neural system", preprint, 2003.

[5] S.A. Campbell and Y. Yuan, "Patterns of oscillations in a ring of identical cells with delayed coupling", in preparation, 2004.

[6] M. Cohen and S. Grossberg, "Absolute stability of global pattern formation and parallel memory storage by competitive neural networks", *IEEE Trans. Systems Man Cybernet.* **13**(5), 815–826, 1983.

[7] B. Ermentrout, "Simulating, analyzing, and animating dynamical systems: A guide to XPPAUT for researchers and students", SIAM, Philadelphia, 2002.

[8] T. Faria and L. Magalhães, "Normal Forms for Retarded Functional Differential Equations with Parameters and Applications to Hopf Bifurcation", *J. Differential Equations* **122**, 181–200, 1995.

[9] M. Golubitsky, I. Stewart and D.G. Schaeffer, *Singularities and groups in bifurcation theory, Vol. II*, Springer-Verlag, New York, 1988.

[10] S. Grossberg, "Competition, decision, and consensus", *J. Math. Anal. Appl.* **66**(2), 470–493, 1978.

[11] S. Grossberg, "Biological competition: Decision rules, pattern formation, and oscillations", *Proc. Nat. Acad. Sci. U.S.A.* **77**(4), 2338–2342, 1980.

[12] J. Guckenheimer and P.J. Holmes, *Nonlinear oscillations, dynamical systems and bifurcations of vector fields*, Springer-Verlag, New York, 1983.

[13] J.K. Hale, "Flows on center manifolds for scalar functional differential equations", *Proc. Roy. Soc. Edinburgh* **101A** 193–201, 1985.

[14] J.K. Hale and S.M. Verduyn Lunel, *Introduction to functional differential equations* Springer-Verlag, New York, 1993.

[15] J.J. Hopfield, "Neurons with graded response have collective computational properties like those of two-state neurons", *Proc. Nat. Acad. Sci. U.S.A.* **81**, 3088–3092, 1984.

[16] J.J. Hopfield, "Neural networks and physical systems with emergent collective computational abilities", *Proc. Nat. Acad. Sci. U.S.A.* **79**, 2554–2558, 1982.

[17] V.B. Kolmanovskii and V.R. Nosov, *Stability of functional differential equations*, Academic Press, 1986.

[18] W. Krawcewicz, P. Vivi and J. Wu, "Computation formulae of an equivariant degree with applications to symmetric bifurcations", *Nonlinear Studies* **4**(1), 89–119, 1997.

[19] W. Krawcewicz and J. Wu, "Theory and applications of Hopf bifurcations in symmetric functional-differential equations", *Nonlinear Analysis* **35** 845–870, 1999.

[20] C.M. Marcus, F.R. Waugh and R.M. Westervelt, "Nonlinear dynamics and stability of analog neural networks", *Physica D* **51**, 234–247, 1991.

[21] C.M. Marcus and R.M. Westervelt, "Stability of analog neural networks with delay", *Phys. Rev. A* **39**, 347–359, 1989.

[22] I. Ncube, S.A. Campbell, and J. Wu, "Change in criticality of synchronous Hopf bifurcation in a multiple-delayed neural system," in *Dynamical Systems and Their Applications to Biology*, S. Ruan, G.S.K. Wolkowicz and J. Wu eds, Fields Institute Communications Vol. 36, 179–193, AMS, 2003.

[23] L.P. Shayer and S.A. Campbell, "Stability, bifurcation and multistability in a system of two coupled neurons with multiple time delays," *SIAM J. Applied Mathematics*, **61 (2)**, 673–700, 2000.

[24] P. van den Driessche, J. Wu and X. Zou, " Stabilization role of inhibitory self-connections in a delayed neural network ," *Physica D.*, **150** 84–90, 2001.

[25] W. Wischert and A. Wunderlin and A. Pelster and M. Olivier and J. Groslambert, "Delay-induced instabilities in nonlinear feedback systems", *Phys. Rev. E*, **49** 203–219, 1994.

[26] J. Wu, "Symmetric functional-differential equations and neural networks with memory", *Trans. Amer. Math. Soc.* **350**(12), 4799–4838, 1998.

[27] J. Wu, T. Faria, and Y.S. Huang, "Synchronization and stable phase-locking in a network of neurons with memory, " *Math. Comp. Modeling*, **30**, 117–138, 1999.